Direct binding of the Kex2p cytosolic tail to the VHS domain of yeast Gga2p facilitates TGN to prevacuolar compartment transport and is regulated by phosphorylation

Mithu De*, Mohamed E. Abazeed*,†, and Robert S. Fuller
Department of Biological Chemistry, University of Michigan, Ann Arbor, MI 48109

ABSTRACT Human Golgi-localized, γ-ear–containing, ADP-ribosylation factor–binding proteins (Ggas) bind directly to acidic dileucine sorting motifs in the cytosolic tails (C-tails) of intracellular receptors. Despite evidence for a role in recruiting ubiquitinated cargo, it remains unclear whether yeast Ggas also function by binding peptide-sorting signals directly. Two-hybrid analysis shows that the Gga1p and Gga2p Vps27, Hrs, Stam (VHS) domains both bind a site in the Kex2p C-tail and that the Gga2p VHS domain binds a site in the Vps10p C-tail. Binding requires deletion of an apparently autoinhibitory sequence in the Gga2p hinge. Ser_{780} in the Kex2p C-tail is crucial for binding: an Ala substitution blocks but an Asp substitution permits binding. Biochemical assays using purified Gga2p VHS–GGA and TOM1 (GAT) and glutathione *S*-transferase–Kex2p C-tail fusions show that Gga2p binds directly to the Kex2p C-tail, with relative affinities $Asp_{780} > Ser_{780} > Ala_{780}$. Affinity-purified antibody against a peptide containing phospho-Ser_{780} recognizes wild-type Kex2p but not $S_{780}A$ Kex2p, showing that Ser_{780} is phosphorylated in vivo; phosphorylation of Ser_{780} is up-regulated by cell wall–damaging drugs. Finally, mutation of Ser_{780} alters trafficking of Kex2p both in vivo and in cell-free *trans*-Golgi network (TGN)–prevacuolar compartment (PVC) transport. Thus yeast Gga adaptors facilitate TGN–PVC transport by direct binding of noncanonical phosphoregulated Gga-binding sites in cargo molecules.

Monitoring Editor
Akihiko Nakano
RIKEN

Received: Apr 27, 2012
Revised: Dec 11, 2012
Accepted: Dec 12, 2012

This article was published online ahead of print in MBoC in Press (http://www.molbiolcell.org/cgi/doi/10.1091/mbc.E12-04-0322) on December 21, 2012.

*These authors contributed equally to this work.

†Present address: Harvard Radiation Oncology Program, 75 Francis St., Boston, MA 02215.

Address correspondence to: Robert S. Fuller (bfuller@umich.edu).

Abbreviations used: 3AT, 3-aminotriazole; BACE, β-secretase; CD-MPR, cation-dependent mannose-6-phosphate receptor; CI-MPR, cation-independent mannose-6-phosphate receptor; C-tail, cytosolic tail; DPAP, dipeptidyl aminopeptidase; GAE, γ-adaptin ear; GAT, GGA and TOM1; GBS, Gga-binding site; Gga/GGA, Golgi-localized, γ-ear–containing, ADP-ribosylation factor–binding protein; GST, glutathione-*S*-transferase; HA, hemagglutinin; IP, immunoprecipitation; MPR, mannose-6-phosphate receptor; MSS, medium-speed supernatant; PSHA, Pep12Ste13αHA fusion substrate; SHA, Ste13αHA fusion substrate; PVC, prevacuolar compartment; SNARE, soluble *N*-ethylmaleimide-sensitive factor attachment protein receptor; TGN, *trans*-Golgi network; VHS, Vps27, Hrs, Stam.

INTRODUCTION

Steady-state localization of singly spanning transmembrane proteins (the processing peptidases Kex2p and Ste13p and the vacuolar protein sorting receptor, Vps10p) to the yeast *trans*-Golgi network (TGN) depends on cycles of vesicular trafficking between the TGN, the late endosome/prevacuolar compartment (PVC), and maturing late Golgi cisternae (Cooper and Stevens, 1996; Bryant and Stevens, 1997; Brickner and Fuller, 1997). It is believed that these proteins follow a common, retromer-dependent PVC–Golgi retrieval pathway (Seaman *et al.*, 1997; Nothwehr *et al.*, 1999). Signals required for this retrograde transport have been identified in the cytosolic domains (cytosolic tails [C-tails]) of Kex2p, Ste13p, and Vps10p (Wilcox *et al.*, 1992; Nothwehr *et al.*, 1993; Cereghino *et al.*, 1995). In the forward direction, evidence from in vivo and in vitro studies indicates that Vps10p follows a Golgi-localized, γ-ear–containing, ADP-ribosylation factor–binding protein (Gga/GGA)–dependent, AP-1–independent, "direct" pathway from the TGN to the PVC, whereas Kex2p

partitions between this direct pathway and an "indirect," Gga-independent, AP-1–dependent pathway through the early endosome (Hirst *et al.*, 2000; Costaguta *et al.*, 2001; Mullins and Bonifacino, 2001; Sipos *et al.*, 2004; Abazeed and Fuller, 2008). In mammalian cells, GGA-dependent TGN-endosomal sorting was found to require interaction of GGAs with motifs in the C-tails of transmembrane proteins (Bonifacino, 2004). Surprisingly, deletion of the C-tails of Kex2p, Ste13p, Kex1p, and Vps10p resulted in efficient default transport from the TGN to the vacuole rather than to the plasma membrane (Cooper and Bussey, 1992; Roberts *et al.*, 1992; Wilcox *et al.*, 1992; Cereghino *et al.*, 1995). However, the fact that the default pathway required clathrin (Seeger and Payne, 1992; Redding *et al.*, 1996b; Deloche *et al.*, 2001) suggested the involvement of an adaptor in TGN–PVC transport and left open the possibility that TGN–PVC cargo proteins contain signals that normally facilitate their recruitment into transport vesicles at the TGN.

The GGA proteins comprise a family of clathrin adaptors that facilitate clathrin-mediated trafficking of cargo between the TGN and endosome by linking cargo sorting and clathrin lattice assembly at vesicle budding sites (Bonifacino, 2004). The modular organization of GGA proteins into Vps27, Hrs, Stam (VHS), GGA and TOM1 (GAT), hinge, and γ-adaptin ear (GAE) domains permits the coordination of multivalent contacts with the C-tails of cargo, Arf-GTP, clathrin, and accessory protein involved in vesicle formation. Biochemical and structural studies of binding between the mammalian GGA-VHS domains and the C-tails of TGN receptors sortilin and two mannose-6-phosphate receptors (MPRs) provided the first evidence for a direct interaction between GGAs and cargo (Bonifacino, 2004). The key residues in the C-tails of the cation-dependent MPR (CD-MPR), cation-independent MPR (CI-MPR), sortilin, memapsin 2 (β-secretase [BACE]), and low-density-lipoprotein receptor–related protein 3 for binding to the VHS domain of human GGAs were shown to constitute acidic dileucine motifs with the consensus sequence DXXLL (Nielsen *et al.*, 2001; Puertollano *et al.*, 2001; Takatsu *et al.*, 2001; Zhu *et al.*, 2001; He *et al.*, 2002; Misra *et al.*, 2002). Phosphorylation of a Ser residue within or adjacent to the acidic dileucine motif enhanced the binding of CI-MPR, BACE, sorLA, and sortilin C-tail sequences to human GGAs, suggesting a phosphoregulated mechanism for binding and cargo sorting (Kato *et al.*, 2002; He *et al.*, 2003; Cramer *et al.*, 2010). Comparison of the sequences of the yeast Gga proteins to the structures of the mammalian GGAs, however, suggested that the yeast proteins might not be able to bind the classic acidic dileucine motif (Misra *et al.*, 2002). In addition, several studies suggest that sorting of the polytopic membrane proteins Gap1p, Fur4p, Sit1p, and Arn1p involves interaction of covalently bound ubiquitin with the GAT domains of the Gga proteins (Bilodeau *et al.*, 2004; Scott *et al.*, 2004; Kim *et al.*, 2007), leading to the notion that yeast Ggas might exclusively mediate sorting of ubiquitin-modified cargo. Recent work, however, suggested that TGN–PVC trafficking of Arn1p and Gap1p, albeit Gga dependent, is independent of both ubiquitin modification and the Gga GAT domain, although the mechanism is unknown (Deng *et al.*, 2009; Lauwers *et al.*, 2009). Although the C-tails of both Kex2p and Vps10p are highly acidic, they contain no obvious acidic dileucine motifs. No Gga-binding sites (GBSs) have been identified in the C-tails of these proteins, and the direct interaction of GBSs with the VHS domains of the yeast Gga proteins has not been demonstrated.

To characterize the precise role of the yeast Gga proteins in TGN-to-PVC transport of Kex2p and Vps10p, we used a directed, yeast two-hybrid strategy to detect and map GBSs in the Kex2p and Vps10p C-tails that bind to the VHS domains of yeast Gga proteins. We used an in vitro binding assay to demonstrate that the Kex2p GBS binds directly to the VHS domain of Gga2p. Efficient binding required Kex2p C-tail residue Ser_{780}, which we found to be phosphorylated in vivo in response to cell wall–damaging agents. Analysis of the effects of Ala and Asp substitutions on the biochemical binding assay, a cell-free TGN–PVC transport assay, and an in vivo assay for Kex2p localization indicated that phosphorylation favored binding to the Gga2p VHS domain and enhanced TGN–PVC sorting by the direct, Gga-dependent pathway.

RESULTS

Two-hybrid interactions between the C-tail of Kex2p and the VHS domains of Gga1 and 2p

On the basis of the demonstrated role of Gga2p in in vivo and cell-free TGN-to-PVC transport of transmembrane proteins and on the established mechanism of direct cargo selection by mammalian GGAs in facilitating transport, we predicted that the yeast Ggas would bind to sequence elements in the C-tails of yeast cargo proteins. To probe possible yeast cargo–Gga adaptor interactions, we tested the C-tail of Kex2p and full-length and truncated forms of Gga2p for binding using a directed yeast two-hybrid assay (Figure 1). In the two-hybrid assay, the Kex2p C-tail did not interact with full-length Gga2p but showed a strong interaction with the VHS-GAT domains of Gga2p (Figure 1B), suggesting the presence of an inhibitory element C-terminal to the GAT domain (see later discussion). When the VHS and GAT domains of Gga2p were tested individually for interaction with Kex2p, only the VHS domain bound to the Kex2p C-tail (Figure 1C). Moreover, the VHS domain of Gga1p also bound to the Kex2p C-tail (Figure 1C).

The hinge region of Gga2p contains an autoinhibitory sequence

To locate more precisely the inhibitory region of Gga2p, we tested a set of truncations for interaction by yeast two-hybrid analysis (Figure 2A and Supplemental Figure S1). Whereas full-length Gga2p, Gga2p-VHS-GAT-hinge, and C-terminal truncations that ended at positions 455, 440, 425, 410, and 395 of the Gga2p hinge domain failed to bind to the Kex2p C-tail, truncations that ended at positions 380, 365, and 350 did bind. These results indicate that an endpoint of the inhibitory sequence is located between residues 380 and 395. We next determined whether the hinge could interact with the VHS domain *in-trans*. Figure 2B shows that the Gga2p-hinge domain interacted with the Gga2p-VHS domain. Taken together, these results suggest that an internal inhibitory sequence in the hinge region of Gga2p binds to the VHS domain, thereby preventing it from interacting with cargo. Because the GGAs have been reported to be monomeric in the cytosol, this autoinhibition may result from intramolecular rather than intermolecular binding (Dell'Angelica *et al.*, 2000; Hirst *et al.*, 2000). However, two-hybrid analysis indicated that the VHS domain of Gga2p exhibited both a strong homomeric interaction and a strong heteromeric interaction with the Gga1p VHS domain, whereas the Gga1p VHS domain exhibited a weaker homomeric interaction (Supplemental Figure S2). This raises the possibility that homodimerization or heterodimerization through the VHS domains may play a role in Gga function. Direct biochemical binding experiments would be necessary to confirm these apparent autoinhibitory and homomeric interactions and the exclude involvement of other factors in these binding events.

Identification of the Gga-binding site in the Kex2p C-tail

To identify the Gga-binding site (GBS) in the Kex2p C-tail, we constructed and tested truncations of the Kex2p C-tail for binding to

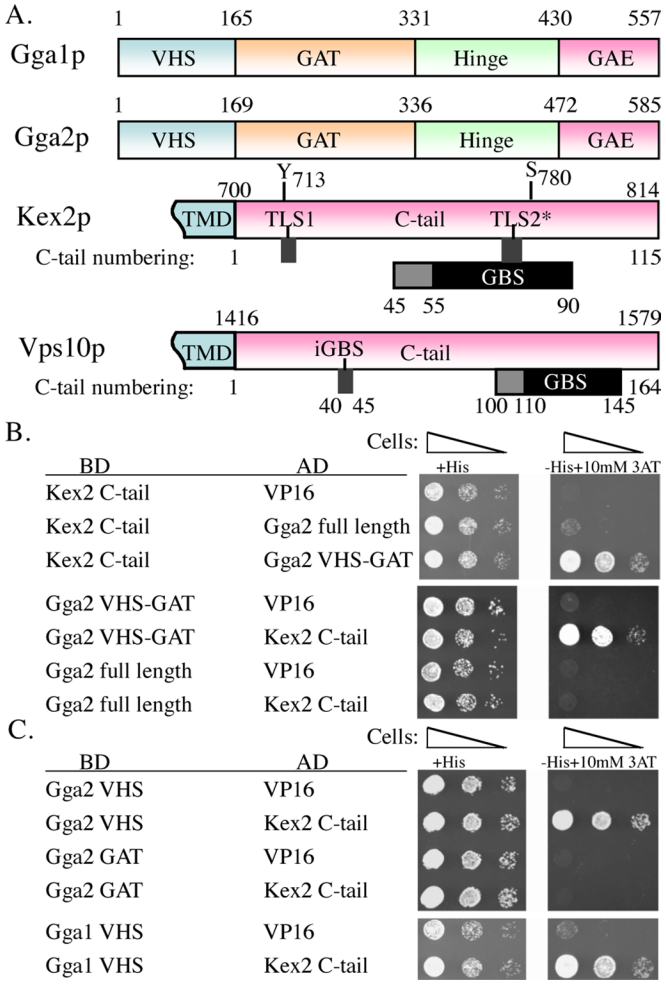

FIGURE 1: Yeast Gga1p and Gga2p VHS domains interact with the C-tail of Kex2p. (A) Shown are 1) operational domain boundaries of Gga1p and Gga2p used in two-hybrid analyses, 2) positions of TLS1, TLS2, and the GBS (Gga-binding site) in the Kex2p C-tail, and 3) positions of the N-terminal boundary (40–45) of the internal inhibitory region and of the GBS in the Vps10p C-tail. (B) Two-hybrid constructs in the LexA-BD (binding domain) and VP16-AD (activation domain) plasmids are indicated by BD and AD, respectively. The regions of Kex2p and Vps10p C-tails within each construct are indicated either by C-tail residue number (1–115, corresponding to residues 700–814 in Kex2p, and 1–164, corresponding to residues 1416–1579 in Vps10p) or, in the case of Tyr_{713} and Ser_{780} in Kex2p, by the position within the overall Kex2p sequence. Full-length Gga2p (1–585) and Gga2p-VHS-GAT (1–336) were used. (C) Gga2p-VHS (1–169), Gga2p-GAT (170–336), and Gga1p-VHS (1x165) two-hybrid constructs in the LexA-BD plasmid were tested for interaction with the full-length Kex2p C-tail (700–814) in the VP16-AD plasmid. (B, C) Strains were spotted at decreasing cell densities on plates that allowed growth without (left, +His) or only with (right, –His + 3 AT) interaction.

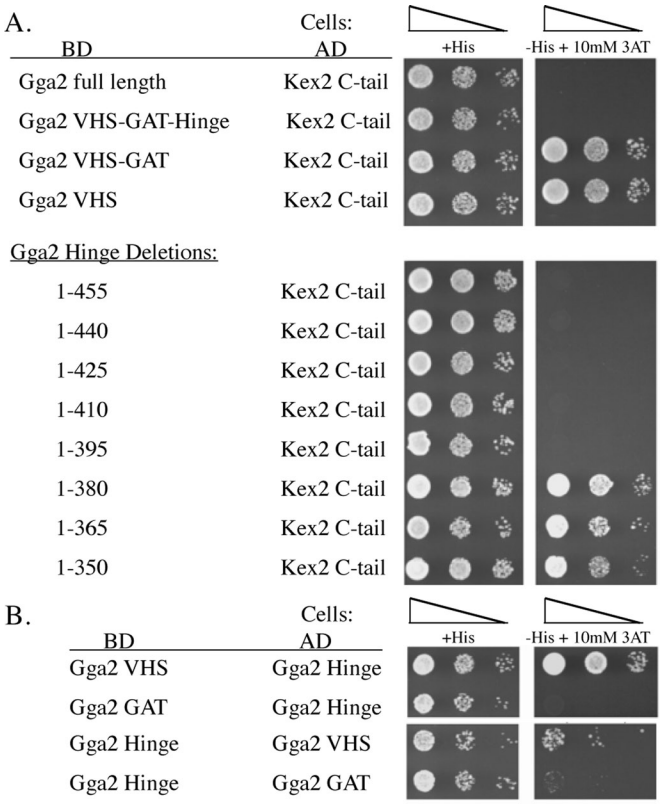

FIGURE 2: Gga2p contains an internal autoinhibitory site that binds its VHS domain. (A) Full-length Gga2p (residues 1–585), Gga2p-VHS-GAT-hinge (residues 1–472), Gga2-VHS-GAT (residues 1–336), and Gga2p-VHS (residues 1–169) in the LexA-BD plasmid and Kex2p C-tail (residues 1–115) in the VP16-AD plasmid were used. C-terminal truncations of Gga2p-VHS-GAT-hinge are indicated by Gga2p residue numbers and were tested in the LexA-BD plasmid for interaction with the Kex2p C-tail (residues 1–115) in the VP16-AD plasmid. (B) Gga2-hinge (residues 337–472) alone binds Gga2-VHS (residues 1–169) and not Gga2-GAT (170–336). Strains were spotted as in Figure 1.

the Gga2p-VHS-GAT domain in the yeast two-hybrid assay (Figure 3, A and B, and Supplemental Figure S3). C-terminal truncations showed strong binding by C-tail residues 1–90 and a sharp loss on truncation to residue 85 (Figure 3A). N-terminal truncations showed strong binding of C-tail residues 45–115, diminished binding with 50–115, and 55–115, and loss of binding with 60–115. These results suggested that strong binding required C-tail residues 45–90 and that essential binding determinants lay within residues 55–90 (Figure 3B). Consistent with this conclusion, Kex2p C-tail residues 45–90 alone interacted with Gga2p-VHS-GAT as well as the full-length C-tail did (Figure 3C), confirming that this region was sufficient for binding to the Gga2p VHS domain.

To identify individual residues critical for binding, we performed alanine scanning mutagenesis (Figure 3D). Simultaneous mutation of Phe_{779} and Ser_{780} to Ala abrogated binding. Single-Ala substitution for Phe_{779} had only a small effect, whereas the $S_{780}A$ mutation nearly eliminated binding (Figure 3E). In contrast, substitution of Asp for Ser_{780} resulted in an interaction comparable to that seen with the wild-type (WT) sequence, suggesting a role for phosphorylation of S_{780} in binding the Gga2p VHS domain.

Two-hybrid interaction between the C-tail of Vps10p and Gga2p

Because yeast two-hybrid analysis showed that the Kex2p C-tail interacted with the Gga2p VHS domain, we asked whether a similar interaction would be observed with the Vps10p C-tail. As shown in Figure 4A and Supplemental Figure S4, full-length Vps10p C-tail did not interact with Gga2p-VHS-GAT. N-terminal truncation of Vps10p C-tail sequences revealed that, whereas a construct containing tail residues 40–164 did not bind, a construct containing tail residues 45–164 did, indicating the N-terminal endpoint of an inhibitory

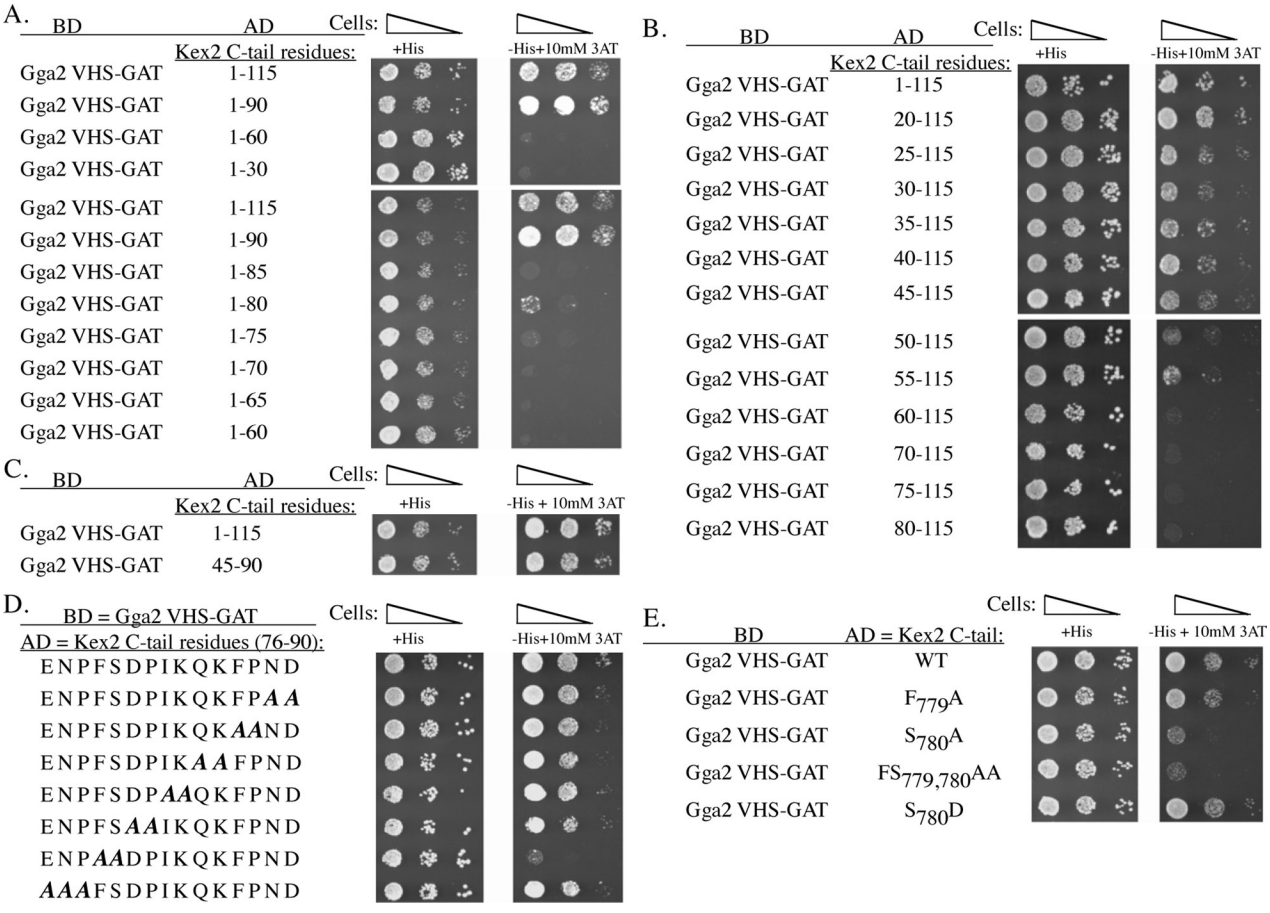

FIGURE 3: Delimiting the Gga-binding site of Kex2p by mutational analysis. (A) C-terminal and (B) N-terminal truncation mutants of Kex2p (C-tail) in the VP16-AD plasmid were tested for interaction with Gga2-VHS-GAT (residues 1–336) in the LexA-BD plasmid. (C) Kex2p C-tail construct expressing residues 45–90 (i.e., Kex2p residues 746-791) in the VP16-AD plasmid was tested for interaction with Gga2-VHS-GAT (residues 1–336) in the LexA-BD plasmid. (D) Ala-scanning mutations in the full-length Kex2p C-tail in the VP16-AD two-hybrid plasmid were tested for interaction with Gga2-VHS-GAT (residues 1–336) in the LexA-BD plasmid. (E) Single-Ala mutations of F_{779} and S_{780}, double-Ala mutations of $F_{779}S_{780}$, and the $S_{780}D$ mutation, all in the full-length Kex2p C-tail in the VP16-AD plasmid, were tested for interaction with Gga2-VHS-GAT (residues 1–336) in the LexA-BD plasmid. The regions of Kex2p C-tail within each construct are indicated by C-tail residue number. Strains were spotted as in Figure 1.

sequence between tail residues 40 and 45. To identify the minimal requirement for Gga2p binding, we tested additional N- and C-terminal truncation mutants (Figure 4, A and B). Vps10p C-tail residues 55–164 showed full binding, which was diminished in a 55–140 construct and lost in a 55–125 construct. Conversely, residues 100–164 showed full binding, which was diminished in a 110–164 construct and lost in a 125–164 construct. These results suggested that primary determinants for binding lay between 110 and 140, although a slightly extended sequence might be needed for full binding. Consistent with these expectations, Vps10p C-tail residues 100–145 alone interacted with Gga2p-VHS-GAT nearly as well as with residues 55–164 (Figure 4C), indicating that this region is sufficient for binding to Gga2p. Finally, the Vps10p C-tail, like that of Kex2p, interacted specifically with the VHS domain of Gga2p (Figure 4D).

Kex2p is phosphorylated at Ser_{780} in vivo

To determine whether Ser_{780} in Kex2p is phosphorylated, we raised a rabbit antibody (anti–P-Ser_{780}) against a synthetic peptide corresponding to Kex2p C-tail residues from Leu_{773} to Phe_{787} and containing phospho-Ser at the position corresponding to Ser_{780}. Glass bead lysates from *kex2*Δ strain CBO17 containing plasmids overexpressing either WT Kex2p (pG5-KX22) or the $S_{780}A$ mutant of Kex2p (pG5-KX22-$S_{780}A$) were analyzed by immunoblotting. When blots were probed with anti–P-Ser_{780} serum, a band corresponding to Kex2p at 135 kDa (along with numerous background bands) was seen in the lanes containing WT Kex2p or $S_{780}A$ Kex2p (Figure 5A, lanes 3 and 4). Competition by unphosphorylated peptide NPP eliminated the $S_{780}A$ Kex2p band but only reduced the WT Kex2p (Figure 5A, lanes 5 and 6). Competition by the phosphorylated peptide PP2 eliminated both the WT and $S_{780}A$ Kex2p bands (Figure 5A, lanes 7 and 8), implying that a component of the antiserum was specific for P-Ser_{780}. Affinity-purified anti–P-Ser_{780} antibody (hereafter, anti–P-Ser_{780} antibody) gave a clearer result. Whereas affinity-purified anti-Kex2p C-tail antibody (hereafter, anti-Kex2p antibody) recognized the WT and $S_{780}A$ Kex2p equally well (Figure 5A, lanes 1 and 2), anti–P-Ser_{780} antibody gave a fourfold stronger signal with WT than with $S_{780}A$ Kex2p (Figure 5A, lanes 9 and 10). On reuse, reactivity of the affinity-purified probe with $S_{780}A$-Kex2p was completely lost, whereas reactivity with WT Kex2p remained (e.g., compare lanes 1–5 with

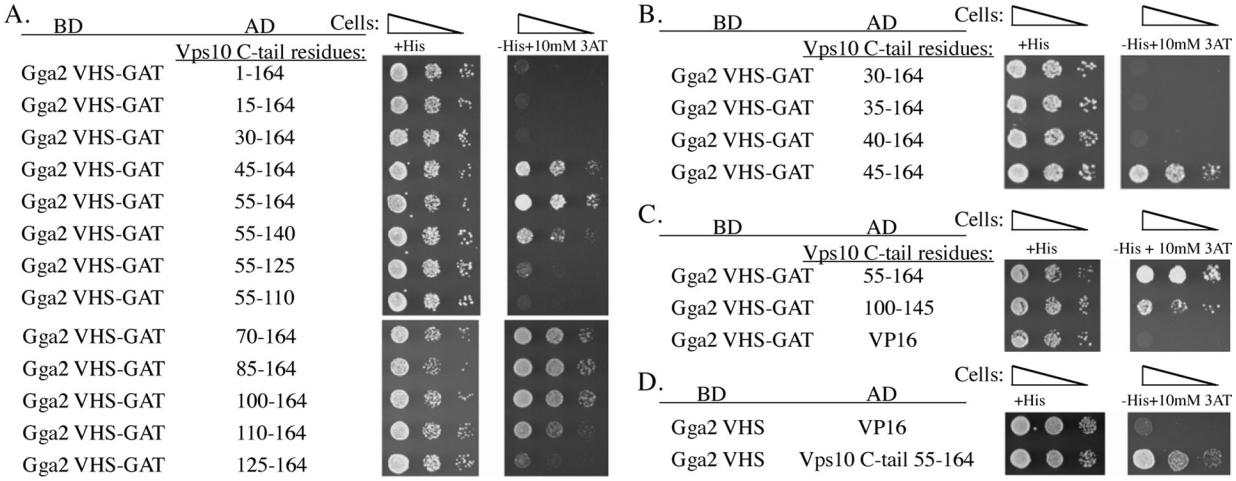

FIGURE 4: The C-tail of Vps10p contains a GBS that interacts with the Gga2p VHS domain. Two-hybrid constructs in the LexA-BD plasmid and the VP16-AD plasmid were as indicated. The regions of Vps10p C-tail within each construct are indicated by C-tail residue number. Gga2-VHS-GAT (residues 1–336) and Gga2-VHS (residues 1–169) were used. (A) A GBS in the Vps10p tail is revealed after deletion of an inhibitory sequence. (B) Fine deletion analysis of the N-terminal end of the inhibitory sequence. (C) Minimal GBS in Vps10p C-tail. (D) The Vps10p GBS binds the Gga2p VHS domain. Strains were spotted as in Figure 1.

lanes 6–9 in Figure 5C), making the anti-P-Ser$_{780}$ antibody an effective reagent for detecting P-Ser$_{780}$ Kex2p. Incubation of extracts containing WT Kex2p with alkaline phosphatase eliminated reactivity with the anti-P-Ser$_{780}$ antibody but not the anti-Kex2p antibody in immunoblots, confirming the specificity of the anti-P-Ser$_{780}$ antibody for Kex2p phosphorylated at Ser$_{780}$ (Supplemental Figure S5).

The experiments in Figure 5A were conducted using a strain overexpressing WT and mutant Kex2p. To ensure that phosphorylation of Ser$_{780}$ was not an artifact of overexpression, we tested reactivity of affinity-purified anti-P-Ser$_{780}$ antibody with WT and S$_{780}$A Kex2p expressed at a range of levels from the WT level to ~150 times the WT level (Figure 5B). WT Kex2p was detected by anti–P-Ser$_{780}$ antibody when expressed at the WT level and overexpressed at 25 and 150 times the WT level (Figure 5B). Judged by the ratio of the anti–C-tail signal to the anti-P-Ser$_{780}$ signal, the degree of phosphorylation was highest at the WT level of expression (3.4:1) and was diminished with overexpression (5:1 for 25 times; 19:1 for 150 times). This may reflect the fact that overexpression of Kex2p results in mislocalization, with 150-times overexpression resulting in accumulation of Kex2p in aberrant membrane–enclosed structures (Wilcox *et al*. 1992).

Kex2p function has been tied to the processing of numerous cell wall proteins and enzymes (Mrsa *et al*., 1997; Moukadiri *et al*., 1999; Tomishige *et al*., 2003). To determine whether phosphorylation of Ser$_{780}$ in the Kex2p C-tail is regulated by cell wall damage–response pathways, we examined the effects of cell wall–damaging agents on phosphorylation in cells expressing WT Kex2p or overexpressing WT or S$_{780}$A Kex2p. Treatment of cells overexpressing WT Kex2p with calcofluor white, caffeine, and Congo red for 4 h (Figure 5C, top) or overnight (Supplemental Figure S5) increased phosphorylation of WT Kex2p by twofold to threefold, as measured by immunoblotting with the anti–P-Ser$_{780}$ antibody, relative to the untreated control. Blotting with anti-Kex2 antibody demonstrated that none of these treatments significantly altered the level of Kex2p itself (shown for 4-h treatment, Figure 5C, bottom). WT Kex2p expressed at the WT level also exhibited enhanced phosphorylation after treatment with caffeine for 4 h (1.9-fold), as well as on growth to high density overnight (3.2-fold), a treatment that has been shown to induce the cell wall–integrity pathways (Figure 5D). Enhancement of phosphorylation under these conditions was reproducible, but the degree of enhancement was variable because of variation of baseline phosphorylation of WT Kex2p (Supplemental Figure S6B). These results suggest that phosphorylation of the Kex2p cytosolic tail reflects physiological regulation of trafficking of the protein.

Direct binding of the Kex2p C-tail to Gga2p VHS-GAT

To determine whether the binding of the Kex2p C-tail to the Gga2-VHS domain was direct, we carried out binding assays using glutathione *S*-transferase (GST)–Kex2p C-tail and C-terminally hexahistidine (His$_6$)-tagged Gga2p-VHS-GAT expressed in and purified from *Escherichia coli* (Figure 6). The VHS-GAT-His$_6$ construct was used because the GST-VHS construct could not be purified in good yield. GST-Kex2p C-tail fusion protein bound to glutathione–agarose retained purified VHS-GAT-His$_6$, with the VHS-GAT-His$_6$–bound fraction increasing as a function of the amount of its input (Figure 6A). This interaction was inhibited by incubation with increasing amounts of purified, untagged VHS-GAT (Figure 6A). Moreover, consistent with yeast two-hybrid data, the binding assay also showed that Kex2p C-tail residues 45–90 alone were capable of retaining Gga2-VHS-GAT-His$_6$ (Figure 6B). Taken together, these results suggest a direct and specific interaction between the Kex2p C-tail and Gga2-VHS-GAT-His$_6$. Directed yeast two-hybrid data indicated that substitution of Ala for Ser$_{780}$ reduced binding of the Kex2p C-tail to the Gga2p VHS domain and that the phosphomimetic substitution of Asp for Ser$_{780}$ permitted a strong interaction with the Gga2p VHS domain (Figure 3E). To determine how the nature of the residue at position 780 affected direct binding of the Kex2p C-tail to the Gga2p VHS domain, we tested purified WT, S$_{780}$A, and S$_{780}$D GST-Kex2p C-tail fusion proteins for binding to purified Gga2p VHS-GAT-His$_6$. The S$_{780}$A-Kex2p C-tail exhibited twofold lower binding and the S$_{780}$D-Kex2p C-tail exhibited twofold higher binding than the WT tail (Figure 6C). Pretreatment of the WT GST-Kex2p C-tail fusion and the S$_{780}$D GST-Kex2p C-tail fusion with the anti–P-Ser$_{780}$ antibody reduced binding of purified Gga2p VHS-GAT-His$_6$ by more

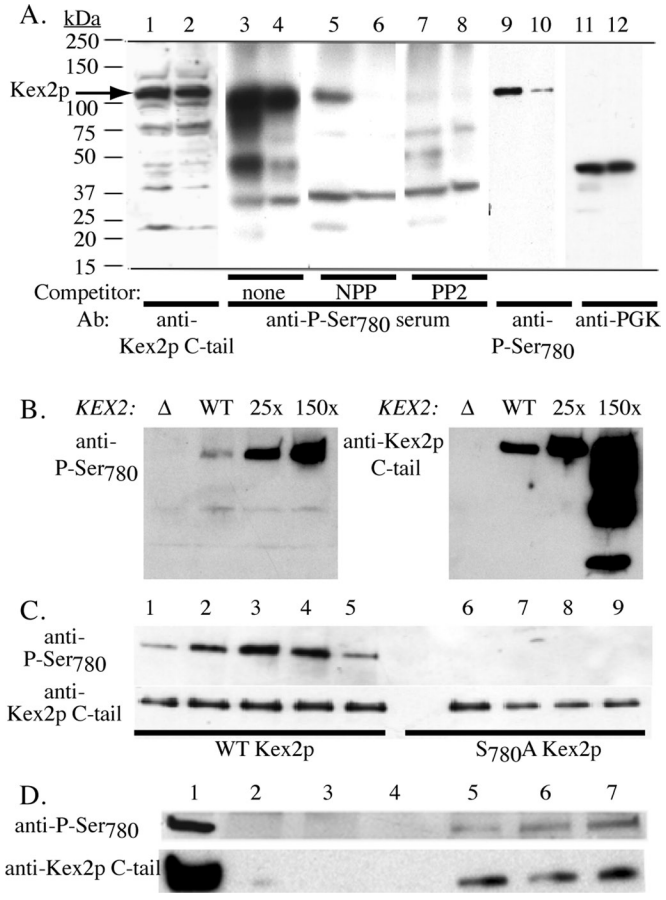

FIGURE 5: Kex2p Ser_{780} is phosphorylated in vivo, and phosphorylation is increased under conditions of cell wall damage. (A) WT Kex2p is phosphorylated at S_{780} in vivo. After glass bead lysis of CBO17 cells containing pG5-KX22 (WT Kex2p, odd-numbered lanes) or pG5-KX22-S_{780}A (S_{780}A-Kex2p, even-numbered lanes), cell extracts were analyzed by immunoblotting with anti-Kex2p antibody (lanes 1 and 2), anti–P-Ser_{780} serum (lanes 3–8), anti–P-Ser_{780} antibody (lanes 9 and 10), or anti–yeast phosphoglycerate kinase antibody (lanes 11 and 12). Lanes 3 and 4 contained no competing peptide, lanes 5 and 6 contained competing NPP, and lanes 7 and 8 contained competing PP2. Measurement of membrane-associated Kex2 proteolytic activity (Brenner and Fuller, 1992) confirmed the presence of equivalent amounts of WT and Ser_{780}A Kex2p. (B) Kex2p expressed at its WT level is phosphorylated at Ser_{780}. Extracts of *kex2*Δ strain CBO16 (Δ), *KEX2* WT strain CBO18, or *kex2*Δ strain CBO17 containing YCpKX22 (25×) or pG5-KX22 (150×) were analyzed by immunoblotting with anti–P-Ser_{780} antibody (left) or anti-Kex2p antibody (right). (C) CBO17 containing YCpKX22 (lanes 1–5) or YCpKX22-S_{780}A (lanes 6–9) was grown to log phase (lane 1 and 6) and then grown for 4 h in the presence of calcofluor white (lanes 2 and 7), caffeine (lanes 3 and 8), Congo red (lanes 4 and 9), or no drug (lane 5). Lysates were analyzed by immunoblotting with anti–P-Ser_{780} antibody (top) or anti-Kex2p antibody (bottom). The slight reduction of S_{780}A Kex2p seen here in stressed cells was not a reproducible result. (D) *kex2*Δ strain CBO16 (lanes 2–4) and *KEX2* WT strain CBO18 (lanes 5–7) were grown to log phase (lanes 2 and 5) and treated with caffeine for 4 h (lanes 3 and 6) or grown overnight to high density (lanes 4 and 7). Equal amounts of extracted protein were analyzed by immunoblotting with anti–P-Ser_{780} antibody (top) or anti-Kex2p antibody (bottom). Lane 1 contains extract of CBO17 containing YCpKX22 to provide a marker for the Kex2p band. See *Materials and Methods* for further details.

than 80%, consistent with the conclusion that the epitopes in the Kex2p C-tail recognized by the affinity-purified anti–P-Ser_{780} antibody overlap the binding site for the Gga2p VHS domain (Figure 6D). When phosphorylated (PP2) and nonphosphorylated (NPP) peptides were used as competitors in the binding assay, both reduced retention of purified Gga2p VHS-GAT-His_6, but PP2 was a more efficient competitor (Figure 6E). Measurement of rates of dissociation of Gga2p VHS-GAT-His_6 from resin containing WT, S_{780}D-, and S_{780}A-Kex2p C tails indicated that the relative stability of these Gga2p-VHS-GAT-His_6 complexes was S_{780}D > WT > S_{780}A (Figure 6, F and G). Taken together, these results support the conclusion that the Gga2p VHS domain binds directly to the region within the Kex2p C-tail mapped by the two-hybrid assay and that presence of negative charge (or phosphorylation, as indicated by the competition in Figure 6E) at the position of Ser_{780} directly enhances binding affinity. The K_d values for binding of purified Gga2p VHS-GAT-His_6 to purified GST-Kex2p C-tail fusion proteins, measured by isothermal titration calorimetry (Supplemental Figure S8), were 6.6 (S_{780}D), 10 (WT), and 400 μM (S_{780}A), confirming the relative binding affinities, S_{780}D > WT > S_{780}A, and also the dramatic effect of the Ala substitution at 780 on binding.

Effects of GBS mutations on the cellular trafficking of Kex2p

To determine whether GBS mutations affect trafficking of Kex2p in vivo, we assessed the effects of the mutations on the essential role of Kex2p in processing the yeast mating pheromone precursor pro–α-factor (Figure 7A) and in the rate of vacuolar turnover of Kex2p (Figure 7B; Fuller *et al.*, 1988; Wilcox *et al.*, 1992). The assay in Figure 7A measures the rate of loss of mating competence after shutting off expression of Kex2p. Because the form of Kex2p used contains a Y_{713}A mutation, which inactivates TLS1 and blocks retrieval from the late endosome, the assay measures the relative rate of exit of Kex2p from the pro–α-factor processing compartment(s)/TGN in the absence of recycling from the PVC (Wilcox *et al.*, 1992). Strain MAY15-8B (*MAT*α *kex2*Δ *gga1*Δ), containing WT; Y_{713}A; Y_{713}A, $FS_{779,780}$AA; or Y_{713}A, S_{780}D Kex2p under *GAL1* promoter control, was grown in galactose media, shifted to glucose media at various times to repress transcription, and then tested for the ability to mate with a *MAT***a** tester strain (Figure 7A). As expected (Wilcox *et al.*, 1992), the mating efficiency of cells in which WT Kex2p expression was shut off did not decline substantially over the course of the experiment (Figure 7A), but the mating efficiency of the retrieval-defective Y_{713}A Kex2p began to decline by 4 h after shifting to glucose. In the context of the Y_{713}A tail, the $FS_{779,780}$AA mutation, which blocks or reduces Gga2p binding, decreased the rate of loss of mating competence, whereas the S_{780}D mutation, which enhances Gga binding, accelerated loss of mating competence. These results are consistent with the loss or reduction of Gga-binding reducing the rate of transport of Kex2p from the TGN to the PVC by the direct, Gga-dependent pathway. In contrast, enhancing Gga-binding by the phosphomimetic S_{780}D mutation appears to increase the rate of transport of Kex2p from the TGN to the PVC by this pathway. In the context of the Y_{713}A mutation, the rate of Kex2p turnover measures the overall rate of transport to the vacuole (Wilcox *et al.*, 1992). Half-lives of WT and mutant forms of Kex2p were measured (Figure 7B) using a *GAL1* promoter shut-off protocol similar to that used in Figure 7A. As expected, WT Kex2p was long lived ($t_{1/2}$ = 330 min), whereas the Y_{713}A mutation resulted in rapid turnover ($t_{1/2}$ = 20 min). In the context of the Y_{713}A mutation, the $FS_{779,780}$AA reduced ($t_{1/2}$ = 26 min), whereas the S_{780}D mutation markedly increased ($t_{1/2}$ < 7.1 min), the rate of vacuolar turnover. The rate measured here for vacuolar delivery of Y_{713}A, S_{780}D Kex2p

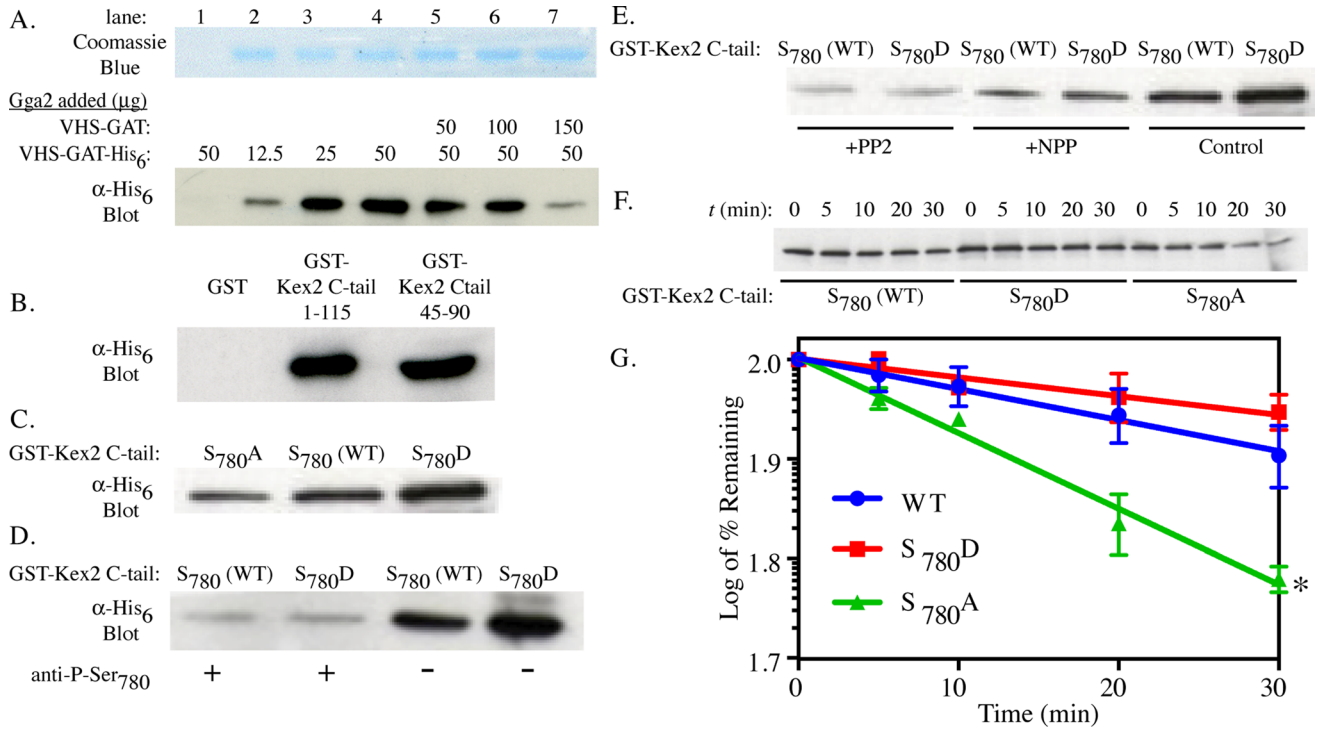

FIGURE 6: Direct binding of yeast Gga2p VHS-GAT-His_6 to the GBS in the Kex2p C-tail. Binding assays were performed as described in *Materials and Methods*. (A) Binding of His_6-Gga2p-VHS-GAT (12.5, 25, 50 μg/ml) to the WT GST-Kex2p C-tail fusion protein (100 μg/ml) in the absence or presence of indicated amounts of untagged VHS-GAT was performed at 4°C. The GST fusion protein was visualized by Coomassie blue staining after SDS–PAGE, and bound His_6-VHS-GAT was detected by immunoblotting with antibody to His_6. (B) Binding of His_6-VHS-GAT (50 μg/ml) with GST (100 μg/ml), a GST fusion protein bearing the C-tail of Kex2p (100 μg/ml), or a GST fusion protein bearing Kex2p C-tail residues 45–90. Bound His_6-VHS-GAT was detected by immunoblotting with antibody to His_6. Binding was performed at 4°C. (C) Binding of His_6-VHS-GAT to WT, $S_{780}A$, and $S_{780}D$ GST-Kex2p C-tail fusion proteins. Binding was performed at RT. (D) Preincubation of GST-Kex2p C-tail fusions with anti–P-Ser_{780} antibody inhibits binding of Gga2p VHS-GAT-His_6. Preincubations with antibody and binding reactions were both performed at RT. (E) Effects of preincubating Gga2p VHS-GAT-His_6 with phosphorylated peptide (PP2) and nonphosphorylated peptide (NPP) on binding to the WT and $S_{780}D$ GST-Kex2p C-tail fusions. Preincubations with peptides and binding assays were both performed at RT. (F) Dissociation of Gga2p VHS-GAT-His_6 from WT, $S_{780}A$, and $S_{780}D$ GST-Kex2p C-tail fusions, a representative experiment. Incubations were performed at RT. (G) Quantification of dissociation rates. Data represent the average of two independent assays, including the one shown in F. Error bars, SE of the mean. The asterisk indicates that the difference between $S_{780}A$ Kex2p and either WT or $S_{780}D$ Kex2p at 30 min is statistically significant ($p < 0.05$, unpaired *t* test). The data are fitted to a first-order decay curve (Prism; GraphPad Software, La Jolla, CA) with $t_{1/2}$ values of 160 min ($S_{780}D$), 97 min (WT), and 40 min ($S_{780}A$) and R^2 values, respectively, of 0.76, 0.83, and 0.97.

is in fact faster than that of Kex2p with a C-tail deletion (11 min; Wilcox *et al.*, 1992). The likeliest explanation for this is that the $S_{780}D$ mutation accelerates delivery of Kex2p from the TGN to the PVC relative to the C-tailΔ protein, which cannot interact with Gga proteins, and that the subsequent delivery of both proteins to the vacuole occurs at the same rate, as each protein lacks a retrieval signal. The data in Figure 7 establish a strong link between the ability of Kex2p to bind Gga and the ability to exit the TGN.

GBS mutations affect cell-free transport of Kex2p from the TGN to the PVC

We previously established an assay that measures transport of Kex2p from the TGN to the late endosome in a cell-free system. This reaction requires Gga2p, clathrin heavy chain, the dynamin homologue Vps1p, the Vps21p rab GTPase, the Vps45p soluble *N*-ethylmaleimide-sensitive factor attachment protein receptor (SNARE) regulator, and the late endosomal t-SNARE Pep12p and measures the delivery of Kex2p from donor TGN membranes to acceptor PVC membranes, where Kex2p cleaves a chimeric substrate, Pep12Ste13αHA fusion substrate (PSHA; for details of the assay see *Materials and Methods* and Blanchette *et al.*, 2004; Abazeed *et al.*, 2005; Abazeed and Fuller, 2008). Transport is measured as the fraction of the total PSHA in acceptor membranes that is cleaved (processed) by Kex2p. With Kex2p in donor membranes, the reaction exhibits two phases: an early, rapid phase (30–40% of the total), which is Gga2p and clathrin independent and most likely represents delivery of Kex2p from early endosomes to the PVC; and a second phase (~60–70% of the total), which is Gga2p and clathrin dependent (Abazeed and Fuller, 2008). This second phase proceeds after a lag of ~10 min and appears to represent direct TGN–PVC transport (Abazeed and Fuller, 2008).

To assess the effects of mutation of S_{780} on cell-free TGN–PVC transport of Kex2p, we prepared donor medium-speed supernatant (MSS) membranes from strains expressing wild-type levels of WT, $S_{780}D$, or $FS_{779,780}AA$ Kex2p. Relative to reactions containing WT Kex2p, reactions containing S_{780D}-Kex2p exhibited an accelerated rate with a reduced lag period, reaching completion at 10 min instead of the more typical 20 min (Figure 8A). Reactions containing

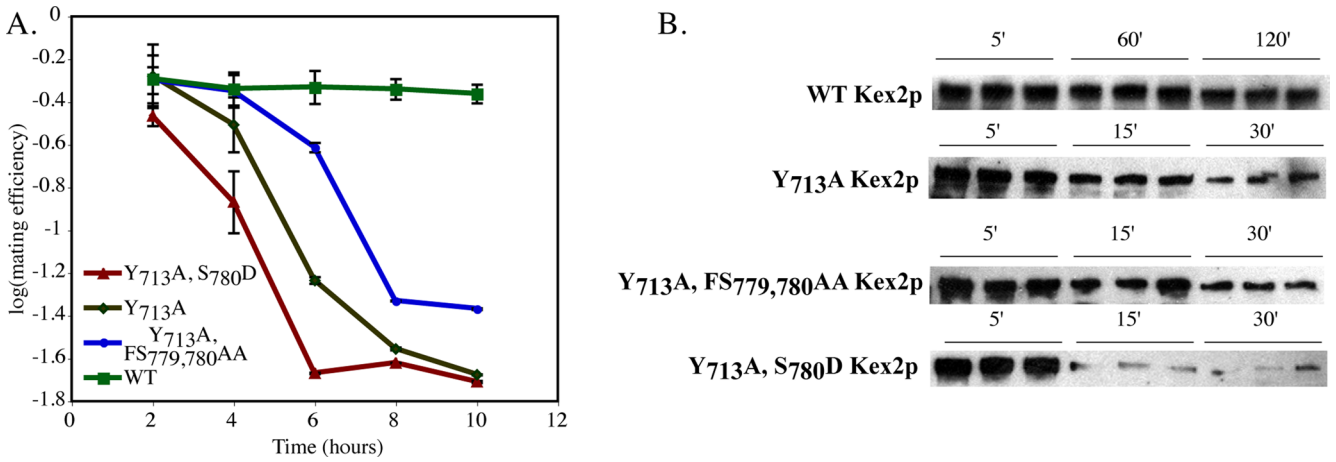

FIGURE 7: Effects of $FS_{779,780}AA$ and $S_{780}D$ mutations on Kex2p localization in vivo. (A) The $FS_{779,780}AA$ mutation suppresses and the $S_{780}D$ mutation enhances the accelerated loss of retrieval-defective $Y_{713}A$-Kex2p from the pro–α-factor processing compartment. Strain MAY15-8B harboring WT and mutant derivatives of *KEX2* under the control of the *GAL1* promoter were grown on galactose for several generations. The strains were then shifted to glucose-containing media to repress expression of the wild-type and mutant *KEX2* constructs. At the indicated time points after the shift to glucose the ability of the cells to mate was measured to generate an index of mating efficiency. Data points represent mean values of duplicates, and the error bars represent the SE. The experiment was performed twice with comparable results. (B) Rates of turnover of WT and $Y_{713}A$, $Y_{713}A$, $FS_{779,780}AA$, and $Y_{713}A$, $S_{780}D$ mutant forms of Kex2p. Turnover experiments were performed as described in *Materials and Methods*. Samples were processed in triplicate at the times indicated. The entire experiment was performed three times with comparable results. Half-lives, calculated by fitting the data in Figure 7B to first-order decay curves using Kaliedagraph (Synergy Software, Reading, PA), were 330 min (WT), 20 min ($Y_{713}A$), 26 min ($Y_{713}A$, $FS_{779,780}AA$), and <7.1 min ($Y_{713}A$, $S_{780}D$).

$FS_{779,780}AA$ Kex2p, in contrast, exhibited a slower rate and more extended lag period than seen with WT Kex2p. All reactions reached the same final extent (~8% PSHA processed), consistent with the fact that the acceptor PSHA membranes were the same in each case. Because the reduced lag seen with S_{780D}-Kex2p raised the possibility that a larger fraction of the reaction might be occurring through the Gga-independent indirect pathway, the dependence of the reactions on Gga2p was assessed. Previously it was shown that reactions using MSS from MAY17—a strain lacking Gga1p and expressing only a form of Gga2p containing a C-terminal 13-myc epitope tag—could be inhibited by anti–c-myc antibody (Abazeed and Fuller, 2008). MSS was prepared from MAY17 expressing wild-type levels of WT, $S_{780}D$, or $FS_{779,780}AA$ Kex2p and tested for transport competence. These membranes exhibited time-course profiles (Supplemental Figure S7A) similar to those seen in Figure 8A using MSS from a *GGA1 GGA2* WT strain. Preincubation of donor MSS with increasing amounts of anti–c-myc antibody resulted in inhibition of reactions with all three forms of Kex2p and indicating that all of the reactions were Gga dependent (Supplemental Figure S7C).

Unexpectedly, when donor MSS membranes were titrated into the reaction, saturation was seen with the 50-μg donor membrane fraction containing WT Kex2p, whereas reactions with donor membranes containing either $S_{780}D$ or $FS_{779,780}AA$ Kex2p required approximately fourfold higher levels of donor membrane to reach saturation (Figure 8B). The same effect was seen with MSS prepared from the *gga1Δ GGA2::13myc* strain MAY17 (Supplemental Figure S7B). Kex2p specific activity was nearly identical in the three MSS preparations, between 100 and 110 U/mg, and consistent with previously measured WT levels of Kex2 activity (Fuller *et al.*, 1989a), so the difference cannot be accounted for by reduced levels of the S_{780} mutant enzyme per se. A possible explanation is that the $S_{780}A$ and $S_{780}D$ mutations localized larger fractions of Kex2 to compartments from which Gga2p-dependent transport could not occur. Because of enhanced Gga2p-binding and TGN exit, $S_{780}D$ Kex2p might be more enriched in the PVC, whereas decreased Gga2p binding and TGN–PVC transport might result in $S_{780}A$-Kex2p enrichment in the early endosome. To test the hypothesis that the S_{780} mutations altered the distribution of Kex2p in TGN/endosomal membranes, we assessed the behavior of donor membranes containing WT and C-tail mutant forms of Kex2p by using the cell-free TGN homotypic fusion reaction (Brickner *et al.* 2001). This assay depends on direct fusion of TGN membranes containing Kex2p with TGN membranes containing the Ste13αHA fusion substrate (SHA) fusion protein, which consists of full-length Ste13p fused to C-terminal Kex2-cleavage site and 3× hemagglutinin (HA) tag. Activity in this assay therefore likely reflects Kex2p levels in the TGN (Figure 9). In contrast to the results with the TGN–PVC assay, both membranes containing $S_{780}D$ and $S_{780}A$ Kex2p showed slower kinetics in the TGN homotypic fusion reaction than membranes containing WT Kex2p, with the $S_{780}D$ Kex2p-containing membranes exhibiting the slowest reaction (Figure 9A). This result is consistent with there being less C-tail mutant Kex2p in the TGN donor compartment. Indeed, in donor membrane titration assays, membranes containing $S_{780}D$ Kex2p showed twofold lower activity than membranes containing WT Kex2p, with $S_{780}A$ Kex2p membranes exhibiting intermediate activity (Figure 9B). These results suggest that both $S_{780}D$ and $S_{780}A$ Kex2p are present at reduced levels in TGN membranes and are thus consistent with mutation of Ser_{780} altering the steady-state distribution of Kex2p. This finding makes it all that much more striking that the $S_{780}D$ mutation renders Kex2p more rapidly recruited into cell-free, Gga-dependent TGN–PVC transport. These results are consistent with the conclusion that phosphorylation of Ser_{780} regulates Kex2p sorting at the TGN by increasing partitioning of Kex2p into the direct, Gga-dependent pathway.

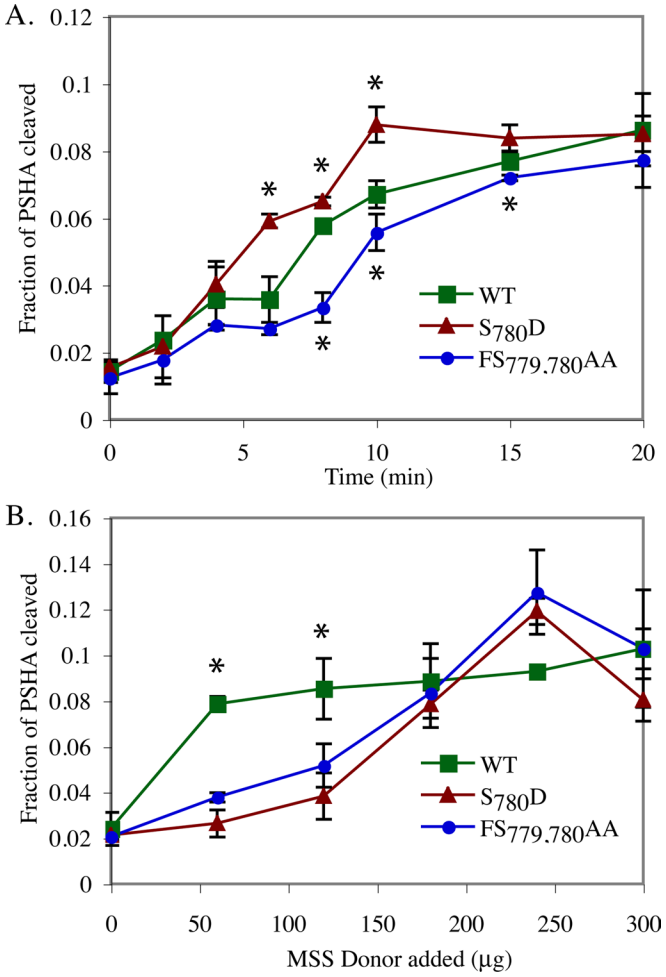

FIGURE 8: The $FS_{779,780}AA$ mutation suppresses and the $S_{780}D$ mutation enhances cell free TGN–PVC transport. Cell-free TGN–PVC transport reactions were conducted using donor MSS from cells expressing WT, $FS_{779,780}AA$, or $S_{780}D$ Kex2p and acceptor MSS from cells expressing the chimeric Kex2p substrate PSHA, which is localized to the PVC. The assay measures the cleavage of PSHA in acceptor PVC membranes by Kex2p delivered from TGN donor membranes. For details see *Materials and Methods*. (A) Time course. (B) Donor MSS titration. Data points represent mean values of triplicates; error bars represent the SD of the mean. Entire experiments were performed three times with comparable results. Asterisks indicate that the difference between the indicated points and points on the other curves were significant ($p < 0.05$, unpaired *t* test).

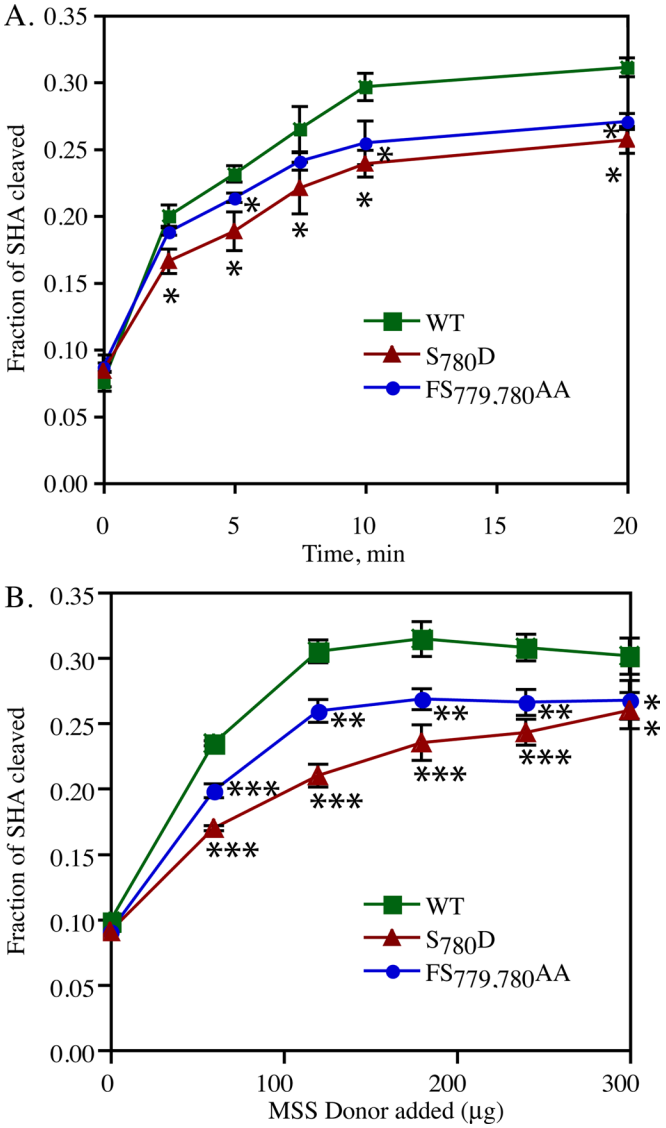

FIGURE 9: Mutation of Ser_{780} reduces Kex2p activity available for TGN homotypic fusion. Cell-free TGN-homotypic fusion reactions were conducted using donor MSS from cells expressing WT, $FS_{779,780}AA$, or $S_{780}D$ Kex2p and acceptor MSS from cells expressing the chimeric Kex2p substrate SHA, which is localized to the TGN. The assay measures the cleavage of SHA in TGN membranes after fusion with TGN membranes containing Kex2p. For details see *Materials and Methods*. (A) Time course. (B) Donor MSS titration. Data points represent mean values of triplicates; error bars represent the SD of the mean. Entire experiments were performed three times with comparable results. The significance (unpaired *t* test) of the difference between the indicated points and WT points was as follows: $*p < 0.05$; $**p < 0.01$; $***p < 0.001$. In B, the difference between values for the two mutants for points from 60 to 240 µg was significant ($p < 0.01$ for 60 and 120 µg and $p < 0.05$ for 180 and 240 µg).

DISCUSSION

Interactions between GBSs in the Kex2p and Vps10p C-tails and Gga proteins and their role in normal TGN–PVC transport

Localization of processing enzymes such as Kex2p and Ste13p to the yeast TGN is a dynamic process achieved by cycles of vesicular trafficking from mature TGN compartments to endosomal compartments and back to maturing Golgi compartments (Brickner and Fuller, 1997; Bryant and Stevens, 1997). Similarly, sorting of soluble enzymes to the vacuole depends on TGN-endosome-Golgi cycling of the Vps10p receptor (Cooper and Stevens, 1996). Although the "retrieval" pathway from the PVC to the Golgi has long been known to require specific sorting signals in the C-tails of these proteins, complete deletion of C-tail sequences from these proteins failed to block efficient TGN-to-PVC trafficking (Wilcox *et al.*, 1992; Nothwehr *et al.*, 1993; Cereghino *et al.*, 1995). Here we showed that despite the existence of this C-tail–independent TGN–PVC transport mechanism, the C-tail sequences in both Kex2p and Vps10p contain sites that interact with the VHS domains of the yeast Gga proteins, the clathrin adaptors required for direct TGN–PVC trafficking. We showed further, in the case of Kex2p, that binding is direct and ubiquitin independent, that it is enhanced by phosphorylation of a

specific site, and that mutations that affect the binding of the Kex2p GBS to purified Gga2p VHS-GAT also affect TGN–PVC trafficking both in vivo and in a cell-free assay. Thus, although TGN–PVC trafficking of singly spanning proteins such as Kex2p and Vps10p can be achieved by default, we propose that it is ordinarily driven through specific, direct, and regulated binding of C-tail sequences to the Gga adaptors.

This direct interaction between cargo-sorting signals and the Gga1/2p VHS domains stands in contrast to the ubiquitin-dependent sorting of several polytopic membrane proteins, in which covalently bound ubiquitin mediates binding to the GAT domain of the Gga proteins (Lauwers *et al.*, 2010). Recent evidence suggests that the ubiquitin–GAT interaction may be required only for Gga-dependent sorting at the PVC into the luminal vesicles of multivesicular endosomes and that other interactions mediate Gga-dependent sorting of polytopic proteins at the TGN (Deng *et al.*, 2009; Lauwers *et al.*, 2009). Whether the ubiquitin-independent interactions at the TGN involve direct binding to the Gga VHS domains remains to be seen.

Potential regulation of Gga-GBS binding by apparent autoinhibitory mechanisms

Detection of the binding of Gga2p to sequences in the Kex2p and Vps10p C-tails required deletion of an internal inhibitory sequence in the Gga2 linker domain that could itself bind to the Gga2p VHS domain. Thus, although recent work called into question the functional significance of autoinhibitory, VHS-binding sequences in the linker regions of mammalian GGA proteins (Cramer *et al.*, 2010), an even more recent study challenged this view (Doray *et al.*, 2012), and our data indicate that this is a property conserved in yeast Gga2p. Furthermore, despite the fact that the hinge regions are poorly conserved between yeast Gga1p and Gga2p (16% identity over 100 residues), the 380–395 deletion interval, which contains the internal Gga2p inhibitory sequence, contains a motif, DLLGD, that is conserved between the two proteins. Although the existence of an autoinhibitory sequence in the Gga1p hinge has not been directly demonstrated, we propose that the DLLGD motif is a reasonable candidate for the internal VHS-binding site. Indeed, Ala scanning indicates that the two Leu residues in this motif are required for autoinhibition (unpublished data). This site resembles neither the typical acidic dileucine motif nor the Kex2p or Vps10p GBS sequences. The only other motif of at least 5 residues conserved between the Gga1p and Gga2p hinge domains, NLIDF (residues 351–355 in Gga2p), has recently been shown to contain overlapping GAE-domain and clathrin-binding motifs. This sequence governs a distinct autoinhibitory mechanism that regulates competing interactions of Gga2p with clathrin and the Ent5p adaptor (Hung *et al.*, 2012). Thus there may be multiple internal mechanisms that regulate the multivalent binding activities of the yeast Gga proteins.

Detection of binding of the Vps10p C-tail to Gga1/2 VHS domains required deletion of membrane-proximal inhibitory sequences in the Vps10p tail. Deletion analysis indicated that the N-terminus of this inhibitory sequence lay between tail residues 40 and 45, which contains a sequence, FYVF, previously shown to regulate Vps10p trafficking (Cereghino *et al.*, 1995; Cooper and Stevens, 1996). Although the mechanism of this inhibition has not been determined, its existence suggests that conformational interactions in the Vps10p tail might be important in regulating exposure of sorting determinants.

Nature of the GBS in the Kex2p and Vps10p C-tails

As determined by the two-hybrid assay, the minimal GBS sequence in Kex2p comprised ~36 residues (C-tail residues 55–90; Supplemental Figure S3) and in Vps10p comprised ~31 residues (C-tail residues 110–140; Supplemental Figure S4). Alanine scanning mutagenesis of the C-terminal side of the Kex2p GBS identified Ser_{780} as an important residue for binding and showed that the identity of residues C-terminal to position 780 was unimportant for binding. Further mutagenesis showed that substitution of Asp for Ser_{780} permitted binding in the two-hybrid assay and suggested that Ser_{780} might be a phosphorylation site (see later discussion). In direct biochemical binding assays, the $S_{780}A$ substitution decreased and the $S_{780}D$ substitution increased the affinity of Gga2 VHS-GAT for the Kex2p GBS. The Ala and Asp substitutions also had opposite effects on TGN–PVC trafficking both in vivo and in a cell-free assay for TGN–PVC transport. The effects of the mutations were shown in vivo using both a sensitive mating assay that measures the rate of loss of Kex2p activity from the pro–α-factor processing compartment, presumably the TGN, and a turnover assay, which measures the overall rate of delivery to the vacuole. In the loss-of-mating-competence assay, the Ala substitution reduced the net rate of exit of Kex2p from the processing compartment, whereas the Asp substitution increased it. In the turnover assay, the $S_{780}A$ substitution decreased and the $S_{780}D$ substitution increased the rate of vacuolar delivery. In the cell-free TGN-PVC assay, the Ala substitution similarly decreased the initial rate of TGN-PVC transport of Kex2p, whereas the Asp substitution increased it. The specificity of the effects of the Asp and Ala substitutions for Ser_{780} is underlined by the fact that both substitutions reduced Kex2p activity available for TGN homotypic fusion. From this we conclude that Ser_{780} is an important determinant for binding to the Gga1/2 VHS domain and that Ser_{780} phosphorylation positively regulates Gga-dependent sorting at the TGN.

However, because the Ala_{780} substitution only reduced but did not eliminate binding, and because it appeared only to reduce rather than eliminate TGN-PVC trafficking in the in vivo and cell-free assays as well, we conclude that sequences on the N-terminal side of the Kex2p GBS are also likely to be important for binding. Although neither the Kex2p nor the Vps10p GBS contains canonical DXXLL Gga-binding motifs, these presumptive VHS-binding sequences contain clusters of acidic and aliphatic residues like the known mammalian VHS-binding sequences. Suggestive alignments can be made both between the Kex2p and Vps10p GBSs and between these GBSs and the Gga-binding sequences of CI-MPR, BACE, sortilin, and SorLA (Supplemental Figure S9). Clustal W alignment of Kex2p and Vps10p C-tails from multiple *Saccharomyces* species aligns a conserved Thr residue in the Vps10p tails with Ser_{780} in Kex2p. In each case, these residues are flanked at their N-terminal side by acidic sequences. An alternative manual alignment of the Kex2p and Vps10p sequences with the mammalian GBS motifs aligns Asp residues in the yeast proteins with the conserved Asp of the mammalian GBS motifs and aligns at least one Leu in each yeast sequence with the conserved aliphatic residues of the mammalian GBS motifs. The crystal structures of these motifs bound to the VHS domain of GGA1 (sortilin, BACE, and SorLA) or GGA3 (CI-M6PR) identify key conserved residues in the mammalian VHS domains that are required for interaction with the Asp and Leu residues (or Asp, Val, and Met residues in the case of SorLA) of the GBS motifs (Misra *et al.*, 2002; Shiba *et al.*, 2002; He *et al.*, 2003; Cramer *et al.*, 2010). As observed by Misra *et al.* (2002), several of these VHS residues are not conserved in the yeast Gga1&2p VHS domains. This is consistent with the VHS domains of the yeast Gga proteins interacting preferentially with yeast GBS motifs that differ from the mammalian GBS motifs.

Regulation of Gga binding by phosphorylation of Ser_{780} in the Kex2p GBS

Phosphorylation of the Kex2p C-tail was reported previously (Brickner, 1998; Johnston *et al.*, 2005). Here, however, we demonstrate the molecular, cellular, and physiological effects of a specific phosphorylation event in the C-tail. Phosphorylation of Ser_{780} in the Kex2p C-tail in vivo was confirmed by the fact that an affinity-purified antibody specific for a peptide containing phospho-Ser_{780} within the Kex2p GBS preferentially recognized WT versus $S_{780}A$ Kex2p in immunoblotting of cell extracts. Biochemical binding assays confirmed that this antibody blocked binding of the Kex2p C-tail to Gga2 VHS-GAT. As indicated earlier, the results of in vivo and in vitro assays indicated that the phosphomimetic substitution of Asp at 780 increased, whereas the Ala substitution decreased, the rate of TGN–PVC transport of Kex2p. As indicated, despite the fact that the Ala substitution completely blocked binding of the Kex2p GBS to the Gga2p VHS domain in the two-hybrid assay, the Ala_{780} Kex2p C-tail still bound to the purified Gga2p VHS-GAT protein, although substantially more weakly than did the WT or Asp_{780} C-tails. This is consistent with a modulatory role for phosphorylation of Ser_{780}, with phosphorylation facilitating Gga-dependent sorting. A modulatory role for phosphorylation would be consistent with the effects of phosphorylation of the C-tails of mammalian proteins on their interactions with mammalian Ggas (Supplemental Figure S9; Cramer *et al.*, 2010).

Unlike Vps10p, which follows only the direct, Gga-dependent pathway to the PVC, Kex2p partitions between this direct pathway and an indirect pathway through the early endosome. We hypothesize that phosphorylation acts as a switch to enhance partitioning into the direct pathway. Evidence supporting this includes the fact that the GBS and Ser_{780} phosphorylation site in the Kex2p C-tail overlaps two other targeting signals (Supplemental Figure S10). First, the motif NPFSD, which includes Ser_{780}, is a site that can mediate Sla1p-dependent endocytosis, although Kex2p is not known to travel to the plasma membrane (Tan *et al.*, 1996; Howard *et al.*, 2002). Second, the sequence TNENP, which lies within the minimal GBS, contains the C-terminal endpoint of TGN-localization signal 2 (TLS2), which operationally functions as a TGN retention signal antagonized by Vps13p function and may represent a signal for TGN-early endosome transport (Brickner and Fuller, 1997). By increasing affinity for Gga2p, phosphorylation of Ser_{780} is predicted to increase transport of Kex2p from the TGN to the PVC by the direct, Gga-dependent pathway and therefore to decrease its trafficking via the Gga-independent pathway through the early endosome, that is, to alter the partitioning of Kex2p through the two pathways. Phosphorylation of the Ste13p N-terminal cytosolic tail at Ser_{13} in the context of the fusion protein A-alkaline phosphatase has also been shown to accelerate trafficking from the TGN to the PVC, although it is not known whether this involves enhancement of trafficking via the direct Gga-dependent pathway (Johnston *et al.*, 2005).

It is not known what kinase is responsible for phosphorylation of Ser_{780}. Indeed, the site does not resemble known phosphorylation sites in yeast proteins, so that an empirical approach will be required to identify the responsible enzyme or enzymes. Regulation of phosphorylation of Ser_{780} by cell cycle–damaging/stressing agents suggests the possibility that alterations in Kex2 trafficking may occur in response to cell wall damage, perhaps to alter the profile of substrates processed by Kex2p. At present, however, there is no known alteration in cleavage of substrates by Kex2 under cell wall damage conditions. However, numerous cell wall proteins undergo processing by Kex2p, and *kex2*-null mutations result in cell wall defects (Mrsa *et al.*, 1997; Moukadiri *et al.*, 1999; Tomishige *et al.*, 2003). Furthermore, null mutations in *KEX2* exhibit synthetic interactions with mutations in the genes encoding yapsins 1 and 2, which have been shown to be required for normal glucan incorporation into the cell wall (Komano and Fuller, 1995; Krysan *et al.*, 2005). Thus it is plausible to hypothesize that alterations in trafficking of Kex2p might be important in adaptation to cell wall stress or damage.

In summary, we have shown that direct interactions occur between peptide-targeting motifs in the C-tails of yeast TGN membrane proteins and the VHS domains of the yeast Gga proteins. These interactions are important for the direct Gga-dependent trafficking between the TGN and PVC in the case of Kex2p. Interaction between the Kex2p C-tail and the Gga proteins can undergo physiological regulation by site-specific phosphorylation that enhances sorting into the direct TGN–PVC pathway.

MATERIALS AND METHODS

Strains and plasmids

Strains used were L40 (MAT**a** his3Δ200 trp1-901 leu2-3, 112 ade2 LYS2::$(lexAop)_4$-HIS3 URA3::$(lexAop)_8$-lacZ GAL4; Vojtek *et al.*, 1993), DC14 (MAT**a** his1), JBY209 (MATα kex2Δ2::hisG dap2::kan^r pep4::HIS3 ste13::LEU2; Brickner *et al.*, 2001), MAY17 (JBY209 gga1Δ GGA2::13myc-TRP1; Abazeed and Fuller, 2008), CBO18 (MAT**a** KEX2 pep4::HIS3 prb::hisG prc::hisG), CBO16 (CBO18 kex2Δ2::TRP1), and CB017 (CBO16 MATα; Wilcox *et al.*, 1992). The diploid strain generated by crossing MAY14 (MATα gga1::TRP1 gga2::HIS3) with KRY24-2A (MAT**a** kex2::LEU2) was sporulated, and tetrads were scored to isolate MAY15-8B (MATα kex2::LEU2 gga1::TRP1). All strains except DC14 were from the W303-1B background and had the following additional genetic markers: ade2-1 can1-100 his3-11,15 leu2-3 trp1-1 ura3-1.

CEN4 URA3 plasmids pCWKX10 and pCWKX20 contain the *KEX2* structural gene under control of the *KEX2* promoter and the yeast *GAL1* promoter, respectively (Wilcox *et al.*, 1992). Overlap-extension PCR was used to generate *Nar*I–*Sal*I fragments containing the substitutions $FS_{779,780}AA$, $S_{780}D$, $Y_{713}A/FS_{779,780}AA$, and $Y_{713}A/S_{780}D$. These fragments were subcloned into pCWKX10 and pCWKX20, replacing the WT *Nar*I–*Sal*I fragment (Wilcox *et al.*, 1992) to create pCWKX10-$FS_{779,780}AA$, pCWKX10-$S_{780}D$, pCWKX20-$FS_{779,780}AA$, and pCWKX20-$S_{780}D$. Plasmid pPSHA (previously referred to as pPEP12-STE13ΔTMDα3xHA or pJB10) encodes the chimeric protein PSHA (Blanchette *et al.*, 2004; Abazeed *et al.*, 2005). Plasmid pSHA (previously termed pSTE13αHA) encodes the chimeric protein Ste13αHA (here termed SHA; Brickner *et al.*, 2001). Yeast two-hybrid plasmids expressing the entire sequences or segments of Gga1p, Gga2p, and the C-tails of Kex2p and Vps10p were made by subcloning PCR fragments encoding the residues indicated in Figures 1–4 and Supplemental Figures S1, S3, and S4 into LexA-BD and VP16-AD vectors as described (Vojtek *et al.*, 1993). Kex2p C-tail sequences 1–115 correspond to residues 700–814 of the *KEX2* open reading frame (Fuller *et al.*, 1989b). Vps10p C-tail sequences 1–164 correspond to residues 1416–1579 of the *VPS10* open reading frame (Cereghino *et al.*, 1995). Sequences were amplified by oligonucleotide primers containing *Bam*HI (5′ primer) and *Not*I (3′ primer) restriction sites and cloned directionally into the LexA-BD and VP16-AD vectors. Alanine-scanning mutations were made by overlap-extension PCR in the full-length Kex2p C-tail and cloned into the VP16-AD vector. Plasmids YCpKX22-$S_{780}A$ and pG5-KX22-$S_{780}A$ were constructed by mutating the codon for Ser at position 780 to Ala (AGT to GCT) in the *KEX2* C-tail in plasmids YCpKX22 and pG5-KX22, respectively. In YCpKX22 and pG5-KX22, the full-length *KEX2* open reading frame is under the control of the *TDH3* promoter in the *URA3 CEN4* plasmid YCp50 (YCpKX22) or the

multicopy 2μ *URA3* vector pG5 (pG5-KX22; Wilcox *et al.*, 1992). Plasmids YCpKX22 and pG5-KX22, respectively, lead to Kex2p expression elevated ~25-fold and ~150-fold relative to WT cells (Wilcox *et al.*, 1992). *E. coli* vectors expressing fusions of GST to WT, Ser_{780}Ala, and Ser_{780}Asp-Kex2p C-tails were constructed by inserting sequences encoding residues 700–814 of the Kex2p C-tail into vector pGEX-KG (Guan and Dixon, 1991), generating, respectively, plasmids pGEX-KG-KXC, pGEX-KG-KXC-S_{780}A, and pGEX-KG-KXC-S_{780}D. An *E. coli* vector expressing a fusion of GST to the VHS-GAT domains of Gga2p was constructed by inserting sequences encoding residues 1–336 of Gga2p into pGEX-KG, generating pGEX-KG-VHS-GAT. In pGEX-KG-VHS-GAT-His_6, sequences encoding a hexahistidine tag were appended to the Gga2p C-terminus. Yeast media were as described (Redding *et al.*, 1996a).

Antibodies and reagents

Anti-HA monoclonal antibody (mAb) 12CA5 and anti–c-myc mAb (9E10) were from Roche Applied Science (Indianapolis, IN). Anti-hexahistidine was from Novus Biologicals (Littleton, CO). Anti-GST antibody was from Zymed Laboratories (San Francisco, CA). Anti–yeast phosphoglycerate kinase antibody was from Invitrogen (Carlsbad, CA). Affinity-purified anti–Kex2 C-tail antibody (anti-Kex2p antibody) was as described (Redding *et al.*, 1991). Anti–phosphopeptide-specific antiserum (anti–P-Ser_{780} serum) and affinity-purified antibody (anti–P-Ser_{780} antibody) were prepared by 21st Century Biochemicals (Marlboro, MA). Briefly, rabbits were immunized with phosphopeptide PP1 (Ac-LeuThrAsnGluAsnProPhe(phospho-Ser)AspProIleLysGlnLys-PheCys-NH_2), corresponding to Kex2p residues 773–787, coupled to keyhole limpet hemocyanin. Affinity purification of serum was conducted by successive chromatography on resins containing nonphosphorylated peptide NPP (Ac-CysLeuThrAsnGluAsnPro-PheSerAspProIleLysGlnLysPhe-NH_2) and phosphopeptide PP2 (Ac-CysThrAsnGluAsnProPhe(phospho-Ser)AspProIleLysGln-LysPhe-NH_2). Horseradish peroxidase–conjugated donkey anti-rabbit secondary antibodies were from Santa Cruz Biotechnology (Santa Cruz, CA). Affinity-purified rabbit anti–mouse immunoglobulin G was from Jackson Immuno Research (West Grove, PA). Glutathione–Sepharose 4B and protein A–Sepharose were from Amersham Biosciences (Piscataway, NJ). Pansorbin was from Calbiochem (San Diego, CA). Bovine α-thrombin was from Haematologic Technologies (Essex Junction, VT). Restriction endonucleases, DNA modification enzymes, and calf intestinal alkaline phosphatase were from New England BioLabs (Beverly, MA). Ala-Pro-MCA was from Bachem Bioscience (King of Prussia, PA). All other chemicals and reagents, unless otherwise indicated, were from Sigma-Aldrich (St. Louis, MO).

Two-hybrid analysis

All two-hybrid assays were performed in strain L40 (Vojtek *et al.*, 1993). Transformants containing the indicated LexA-binding domain (LexA-BD) and VP16-activation domain (VP16-AD) plasmid constructs were analyzed by pronging cells onto synthetic dextrose complete (SDC)-Leu-Trp plates and SDC-Leu-Trp-His plates from 96-well microtiter plates. In cases in which nonspecific transactivation of the His reporter was observed, indicated amounts of 3-aminotriazole were added to -Leu-Trp-His plates.

Analysis of Kex2p Ser_{780} phosphorylation

Cultures (25 ml) grown to log phase in SDC-Ura medium (CBO17 containing plasmid pG5-KX22, pG5-KX22-S_{780}A, YCpKX22, or YCpKX22-S_{780}A) or YPAD medium (CBO16 or CBO18) were harvested by centrifugation, and cells were resuspended in 250 μl of lysis buffer (50 mM Tris-HCl, pH 7.0, 6 M urea, 100 mM dithiothreitol, 10% glycerol, 2% [wt/vol] SDS) containing protease inhibitors (complete EDTA-free mini tablet; Roche Applied Science) and phosphatase inhibitors (10 nM okadaic acid, 200 μM sodium vanadate, 50 μM sodium fluoride) and lysed by vortexing with 0.38 g of 0.5-mm glass beads in 13× 100-mm glass tubes for five 20-s intervals alternating with 20 s on ice. Lysates were centrifuged to remove cell debris, and protein was measured in the supernatant fractions by the Bradford assay (Bio-Rad, Hercules, CA). Lysate protein, 100 μg, was heated in SDS–PAGE sample buffer at 98°C for 5 min and subjected to SDS–PAGE (4–20% gradient gels; Invitrogen, Carlsbad, CA). Gels were transferred to nitrocellulose (GE Healthcare, Waukesha, WI), and immunoblots were probed with anti–P-Ser_{780} serum (1:1000 dilution), anti–P-Ser_{780} antibody (3.3 μg/ml), or anti-Kex2p antibody and developed with secondary antibody and ECL reagents (GE Healthcare); exposures were made using BioMax MR film (Kodak, Rochester, NY). Competition experiments were performed by preincubating 10 ml of diluted anti–P-Ser_{780} serum for 30 min at 4°C with 25 μg of phosphorylated peptide PP1 or nonphosphorylated peptide NPP. To measure the effects of cell wall–damaging drugs, log-phase cultures were diluted in yeast extract/peptone/dextrose (YPD) to an OD_{600} of 0.5, and cell wall–damaging drugs (calcofluor white, 20 mg/ml; Congo red, 200 mg/ml; or caffeine, 6 mM) were added for 4 h or overnight at 30°C (Krysan *et al.*, 2005). For quantification of immunoblots, films of appropriate exposure were scanned to create TIFF files that were analyzed using ImageJ software (National Institutes of Health, Bethesda, MD).

Protein expression

GST-Kex2p C-tail fusions, GST-VHS-GAT, and GST-VHS-GAT-His_6 fusion proteins were expressed in *E. coli* BL21 from their respective plasmids, and the proteins were purified. Four hours prior to harvest, fusion protein expression was induced with 100 mM isopropyl-β-D-thiogalactoside. Extracts prepared from cultures by sonication (three 10-s bursts with intermittent cooling) were cleared by centrifugation (12,000 rpm, 5 min) and then incubated with glutathione–Sepharose 4B beads for 30 min at room temperature. Beads were washed three times with phosphate-buffered saline (PBS; 50 mM sodium phosphate, pH 7.0, 150 mM NaCl) plus 0.05% Tween 20 (10 ml). In the case of GST-Kex2p C-tail fusions and the GST-VHS-GAT fusion, protein was eluted with PBS containing 20 mM glutathione. Eluted fractions were pooled, concentrated, and dialyzed against PBS. GST-VHS-GAT-His_6 beads were washed twice with 1 ml of thrombin cleavage buffer (50 mM Tris-HCl, pH 8.0, 150 mM NaCl, 2.5 mM $CaCl_2$ and 0.1% 2-mercaptoethanol). Fusion protein bound to beads was cleaved by bovine a-thrombin to release VHS-GAT-His_6 (Guan and Dixon, 1991). Thrombin was inactivated with 1 mM phenymethylsulfonyl fluoride, and the soluble fraction and two 1-ml washes of thrombin-treated beads were pooled, concentrated, and dialyzed against PBS.

Kex2p C-tail–binding assays

Binding reactions containing GST-Kex2p C-tails (30 or 100 μg) and indicated concentrations of VHS-GAT-His_6 were conducted in 0.5 ml of binding buffer (50 mM 4-(2-hydroxyethyl)-1-piperazineethanesulfonic acid–KOH, pH 7.5, 150 mM KCl, 1 mM $MgCl_2$, 10% [vol/vol] glycerol, and 0.5 mg/ml bovine serum albumin) for 2 h at 4°C or room temperature (RT), as indicated. Glutathione–Sepharose 4B (25 μl) was added, and incubations were continued for 30 min. Suspensions were transferred to chromatography columns, washed three times with binding buffer, and eluted in SDS–PAGE sample

buffer. Samples were subjected to SDS–PAGE and immunoblotted with anti-His_6 antibody to detect bound VHS-GAT-His_6. Competition with untagged VHS-GAT was measured by adding specified concentrations of purified VHS-GAT to the binding reactions. In antibody-blocking assays, Kex2p C-tail and Kex2p C-tail-S_{780}D (30 µg of each) were preincubated with 60 µg of anti–P-Ser_{780} antibody in 0.5 ml of binding buffer for 30 min at RT before adding VHS-GAT-His_6. Competition with phosphorylated and nonphosphorylated peptide was measured by preincubating peptides (15 µg) with VHS-GAT-His_6 (50 µg) for 30 min at RT in 0.5 ml of binding buffer before adding GST-Kex2 C-tails (30 µg). To determine relative dissociation rates of complexes of GST-Kex2 C-tails with VHS-GAT-His_6, after initial binding incubations at RT, standard reactions were diluted 10-fold with binding buffer and incubated at RT for the indicated times before processing.

Quantitative loss-of-mating-competence assays

Assays for loss of mating competence upon shutting off expression of WT and mutant forms of Kex2p under *GAL1* promoter control were conducted as described (Wilcox *et al.*, 1992). Briefly, MAY-5-8B cells harboring *CEN4 URA3* plasmids encoding WT Kex2p (pCWKX20), Y_{713}A-Kex2p (pCWKX21), Y_{713}A/$FS_{779,780}$AA-Kex2p (pCWKX21-$FS_{779,780}$AA), and Y_{713}A/S_{780D}-Kex2p (pCWKX21-S_{780}D) under the control of the *GAL1* promoter were grown in SC-Ura media containing 2% galactose into log phase at 30°C and were then switched to media (SDC-Ura) containing 2% glucose. After indicated times, ~5×10^6 cells were mixed with ~1×10^7 cells of *MAT***a** mating tester strain DC14, and the mixture was collected on 25-mm HATF filters (Millipore, Bedford, MA). The filters were incubated cell side up on YPD plates at 30°C for 4 h, the cells were resuspended in water, and serial dilutions of matings were plated on SD and SDC-Ura. The number of colonies on the SDC-Ura plates represented total the number of diploids plus *MAT*α cells; the number of colonies on SD plates represented total diploids. Mating efficiency is expressed as the number of diploids divided by the number of diploids plus *MAT*α haploids.

Determination of rates of turnover

MAY15-8B cells containing plasmid pCWKX20, pCWKX21, pCWKX21-$FS_{779,780}$AA, or pCWKX21-S_{780}D were grown in SC-Ura containing 2% galactose to an OD_{600} of 0.3 at 30°C, and glucose was added to 2% to repress KEX2 expression. At the indicated time points, cells were harvested by centrifugation, and glass bead lysates were prepared, subjected to SDS–PAGE, and transferred to nitrocellulose, and immunoblots were probed with anti Kex2p antibodies, developed, and quantified as described earlier (see *Analysis of Kex2p Ser_{780} phosphorylation*).

Cell-free TGN–PVC transport and TGN homotypic fusion assays

The basic cell-free assays for TGN-to-PVC transport and TGN homotypic fusion were as described (Brickner *et al.*, 2001; Blanchette *et al.*, 2004; Abazeed *et al.*, 2005; Abazeed and Fuller, 2008). The TGN–PVC transport assay measures delivery of Kex2p activity from TGN membranes to PVC membranes containing the chimeric Kex2p substrate PSHA. PSHA consists of the entire sequence of the PVC syntaxin Pep12p, which localizes the protein to the PVC, followed by the catalytic domain of the Ste13p dipeptidyl aminopeptidase A (DPAP), a Kex2p cleavage site from pro–α-factor and a triple-HA epitope tag. The TGN homotypic fusion assay measures fusion of TGN membranes containing Kex2p activity with TGN membranes containing the chimeric Kex2p substrate SHA. The SHA chimera lacks the Pep12p sequences found in PSHA and contains the Ste13p C-tail and TMD and is thus localized to the TGN. In both assays, MSS was prepared from semi-intact yeast cells by gentle freeze–thaw lysis of yeast spheroplasts, followed by centrifugation at 13,000 × *g*. MSS prepared under these conditions contains cytosol and late Golgi and endosomal membranes but not endoplasmic reticulum or early Golgi vesicles (Brickner *et al.*, 2001). TGN–PVC transport reactions were performed by combining equal volumes (10 µl) of 1) 3× buffer (containing an ATP-regenerating system), 2) donor MSS, prepared from JBY209 or MAY17 containing pCWKX10 (expressing WT Kex2p), pCWKX10-$FS_{779,780}$AA, or pCWKX10-S_{780}D, and 3) acceptor MSS prepared from JBY209 or MAY17 containing plasmid pPSHA, which expresses the PSHA chimera (Blanchette *et al.*, 2004; Abazeed and Fuller, 2008). For TGN homotypic fusion assays, MSS was prepared from JBY209 containing plasmid pSHA, which expresses the SHA chimera (Brickner *et al.*, 2001). Mixtures were incubated at 30°C for 20 min or indicated times to permit transport to occur and terminated by addition of buffer containing 1% Triton X-100. To determine the extent of cleavage of PSHA or SHA by Kex2p, terminated transport reactions were subjected to immunoprecipitation using anti-HA monoclonal antibody, rabbit anti–mouse immunoglobulin G, and Pansorbin (Brickner *et al.*, 2001). The amount of Ste13 dipeptidyl aminopeptidase activity left in the supernatant of the immunoprecipitation (IP) and of a mock-IP (no anti-HA) was determined using the fluorogenic substrate Ala-Pro-AMC. The extent of transport (PSHA) or fusion (SHA) is expressed as the ratio of DPAP activity in the supernatant fractions from the IP and the mock IP (fraction of PSHA or SHA cleaved). For MSS titration experiments, transport reactions were performed by adding donor MSS containing the indicated amount of protein (measured by Bradford assay). Data points represent mean values of triplicates, and error bars represent the SD of the mean. All reactions presented were performed three times with comparable results. At least two independent preparations of MSS were tested.

ACKNOWLEDGMENTS

We thank Anne Vojtek for expert guidance on two-hybrid assays, Amy Chang for helpful discussions, and Scott Horowitz and Raymond Trievel for assistance with isothermal titration calorimetry. This work was supported in part by National Institutes of Health Grant GM50915 and by generous bridge funding from the Endowment for the Basic Sciences and the Department of Biological Chemistry (R.S.F.), by University of Michigan Medical Scientist Training Program Grant GM0786 (M.E.A.), by Genetics Training Program GM07544 (M.E.A.), by a University of Michigan Rackham Graduate School Predoctoral Fellowship (M.E.A.), and by P30 CA46592 to the University of Michigan Comprehensive Cancer Center.

REFERENCES

Abazeed ME, Blanchette JM, Fuller RS (2005). Cell-free transport from the *trans*-Golgi network to late endosome requires factors involved in formation and consumption of clathrin-coated vesicles. J Biol Chem 280, 4442–4450.

Abazeed ME, Fuller RS (2008). Yeast Golgi-localized, gamma-Ear-containing, ADP-ribosylation factor-binding proteins are but adaptor protein-1 is not required for cell-free transport of membrane proteins from the *trans*-Golgi network to the prevacuolar compartment. Mol Biol Cell 19, 4826–4836.

Bilodeau PS, Winistorfer SC, Allaman MM, Surendhran K, Kearney WR, Robertson AD, Piper RC (2004). The GAT domains of clathrin-associated GGA proteins have two ubiquitin binding motifs. J Biol Chem 279, 54808–54816.

Blanchette JM, Abazeed ME, Fuller RS (2004). Cell-free reconstitution of transport from the *trans*-Golgi network to the late endosome/prevacuolar compartment. J Biol Chem 279, 48767–48773.

Bonifacino JS (2004). The GGA proteins: adaptors on the move. Nat Rev Mol Cell Biol 5, 23–32.
Brenner C, Fuller RS (1992). Structural and enzymatic characterization of a purified prohormone processing enzyme: secreted, soluble Kex2 protease. Proc Natl Acad Sci USA 89, 922–926.
Brickner JH (1998). Characterization of the Mechanism of Localization of Membrane Proteins to the *trans* Golgi Network. PhD Thesis. Palo Alto, CA: Stanford University.
Brickner JH, Blanchette JM, Sipos G, Fuller RS (2001). The Tlg SNARE complex is required for TGN homotypic fusion. J Cell Biol 155, 969–978.
Brickner JH, Fuller RS (1997). SOI1 encodes a novel, conserved protein that promotes TGN-endosomal cycling of Kex2p and other membrane proteins by modulating the function of two TGN localization signals. J Cell Biol 139, 23–36.
Bryant NJ, Stevens TH (1997). Two separate signals act independently to localize a yeast late Golgi membrane protein through a combination of retrieval and retention. J Cell Biol 136, 287–297.
Cereghino JL, Marcusson EG, Emr SD (1995). The cytoplasmic tail domain of the vacuolar protein sorting receptor Vps10p and a subset of VPS gene products regulate receptor stability, function, and localization. Mol Biol Cell 6, 1089–1102.
Cooper A, Bussey H (1992). Yeast Kex1p is a Golgi-associated membrane protein: deletions in a cytoplasmic targeting domain result in mislocalization to the vacuolar membrane. J Cell Biol 119, 1459–1468.
Cooper AA, Stevens TH (1996). Vps10p cycles between the late-Golgi and prevacuolar compartments in its function as the sorting receptor for multiple yeast vacuolar hydrolases. J Cell Biol 133, 529–541.
Costaguta G, Stefan CJ, Bensen ES, Emr SD, Payne GS (2001). Yeast Gga coat proteins function with clathrin in Golgi to endosome transport. Mol Biol Cell 12, 1885–1896.
Cramer JF, Gustafsen C, Behrens MA, Oliveira CL, Pedersen JS, Madsen P, Petersen CM, Thirup SS (2010). GGA autoinhibition revisited. Traffic 11, 259–273.
Dell'Angelica EC, Puertollano R, Mullins C, Aguilar RC, Vargas JD, Hartnell LM, Bonifacino JS (2000). GGAs: a family of ADP ribosylation factor-binding proteins related to adaptors and associated with the Golgi complex. J Cell Biol 149, 81–94.
Deloche O, Yeung BG, Payne GS, Schekman R (2001). Vps10p transport from the *trans*-Golgi network to the endosome is mediated by clathrin-coated vesicles. Mol Biol Cell 12, 475–485.
Deng Y, Guo Y, Watson H, Au WC, Shakoury-Elizeh M, Basrai MA, Bonifacino JS, Philpott CC (2009). Gga2 mediates sequential ubiquitin-independent and ubiquitin-dependent steps in the trafficking of ARN1 from the *trans*-Golgi network to the vacuole. J Biol Chem 284, 23830–23841.
Doray B, Misra S, Qian Y, Brett TJ, Kornfeld S (2012). Do GGA adaptors bind internal DXXLL motifs. Traffic 13, 1315–1325.
Fuller RS, Brake A, Thorner J (1989a). Yeast prohormone processing enzyme (KEX2 gene product) is a Ca2+-dependent serine protease. Proc Natl Acad Sci USA 86, 1434–1438.
Fuller RS, Brake AJ, Thorner J (1989b). Intracellular targeting and structural conservation of a prohormone-processing endoprotease. Science 246, 482–486.
Fuller RS, Sterne RE, Thorner J (1988). Enzymes required for yeast prohormone processing. Annu Rev Physiol 50, 345–362.
Guan KL, Dixon JE (1991). Eukaryotic proteins expressed in *Escherichia coli*: an improved thrombin cleavage and purification procedure of fusion proteins with glutathione *S*-transferase. Anal Biochem 192, 262–267.
He X, Chang WP, Koelsch G, Tang J (2002). Memapsin 2 (beta-secretase) cytosolic domain binds to the VHS domains of GGA1 and GGA2: implications on the endocytosis mechanism of memapsin 2. FEBS Lett 524, 183–187.
He X, Zhu G, Koelsch G, Rodgers KK, Zhang XC, Tang J (2003). Biochemical and structural characterization of the interaction of memapsin 2 (beta-secretase) cytosolic domain with the VHS domain of GGA proteins. Biochemistry 42, 12174–12180.
Hirst J, Lui WW, Bright NA, Totty N, Seaman MN, Robinson MS (2000). A family of proteins with gamma-adaptin and VHS domains that facilitate trafficking between the *trans*-Golgi network and the vacuole/lysosome. J Cell Biol 149, 67–80.
Howard JP, Hutton JL, Olson JM, Payne GS (2002). Sla1p serves as the targeting signal recognition factor for NPFX(1,2)D-mediated endocytosis. J Cell Biol 157, 315–326.
Hung CW, Aoh QL, Joglekar AP, Payne GS, Duncan MC (2012). Adaptor autoregulation promotes coordinated binding within the clathrin coat. J Biol Chem 287, 17398–17407.
Johnston HD, Foote C, Santeford A, Nothwehr SF (2005). Golgi-to-late endosome trafficking of the yeast pheromone processing enzyme Ste13p is regulated by a phosphorylation site in its cytosolic domain. Mol Biol Cell 16, 1456–1468.
Kato Y, Misra S, Puertollano R, Hurley JH, Bonifacino JS (2002). Phosphoregulation of sorting signal-VHS domain interactions by a direct electrostatic mechanism. Nat Struct Biol 9, 532–536.
Kim Y, Deng Y, Philpott CC (2007). GGA2- and ubiquitin-dependent trafficking of Arn1, the ferrichrome transporter of *Saccharomyces cerevisiae*. Mol Biol Cell 18, 1790–1802.
Komano H, Fuller RS (1995). Shared functions in vivo of a glycosyl-phosphatidylinositol-linked aspartyl protease, Mkc7, and the proprotein processing protease Kex2 in yeast. Proc Natl Acad Sci USA 92, 10752–10756.
Krysan DJ, Ting EL, Abeijon C, Kroos L, Fuller RS (2005). Yapsins are a family of aspartyl proteases required for cell wall integrity in *Saccharomyces cerevisiae*. Eukaryot Cell 4, 1364–1374.
Lauwers E, Erpapazoglou Z, Haguenauer-Tsapis R, Andre B (2010). The ubiquitin code of yeast permease trafficking. Trends Cell Biol 20, 196–204.
Lauwers E, Jacob C, Andre B (2009). K63-linked ubiquitin chains as a specific signal for protein sorting into the multivesicular body pathway. J Cell Biol 185, 493–502.
Misra S, Puertollano R, Kato Y, Bonifacino JS, Hurley JH (2002). Structural basis for acidic-cluster-dileucine sorting-signal recognition by VHS domains. Nature 415, 933–937.
Moukadiri I, Jaafar L, Zueco J (1999). Identification of two mannoproteins released from cell walls of a *Saccharomyces cerevisiae* mnn1 mnn9 double mutant by reducing agents. J Bacteriol 181, 4741–4745.
Mrsa V, Seidl T, Gentzsch M, Tanner W (1997). Specific labelling of cell wall proteins by biotinylation. Identification of four covalently linked O-mannosylated proteins of *Saccharomyces cerevisiae*. Yeast 13, 1145–1154.
Mullins C, Bonifacino JS (2001). Structural requirements for function of yeast GGAs in vacuolar protein sorting, alpha-factor maturation, and interactions with clathrin. Mol Cell Biol 21, 7981–7994.
Nielsen MS, Madsen P, Christensen EI, Nykjaer A, Gliemann J, Kasper D, Pohlmann R, Petersen CM (2001). The sortilin cytoplasmic tail conveys Golgi-endosome transport and binds the VHS domain of the GGA2 sorting protein. EMBO J 20, 2180–2190.
Nothwehr SF, Bruinsma P, Strawn LA (1999). Distinct domains within Vps35p mediate the retrieval of two different cargo proteins from the yeast prevacuolar/endosomal compartment. Mol Biol Cell 10, 875–890.
Nothwehr SF, Roberts CJ, Stevens TH (1993). Membrane protein retention in the yeast Golgi apparatus: dipeptidyl aminopeptidase A is retained by a cytoplasmic signal containing aromatic residues. J Cell Biol 121, 1197–1209.
Puertollano R, Aguilar RC, Gorshkova I, Crouch RJ, Bonifacino JS (2001). Sorting of mannose 6-phosphate receptors mediated by the GGAs. Science 292, 1712–1716.
Redding K, Brickner JH, Marschall LG, Nichols JW, Fuller RS (1996a). Allele-specific suppression of a defective *trans*-Golgi network (TGN) localization signal in Kex2p identifies three genes involved in localization of TGN transmembrane proteins. Mol Cell Biol 16, 6208–6217.
Redding K, Holcomb C, Fuller RS (1991). Immunolocalization of Kex2 protease identifies a putative late Golgi compartment in the yeast *Saccharomyces cerevisiae*. J Cell Biol 113, 527–538.
Redding K, Seeger M, Payne GS, Fuller RS (1996b). The effects of clathrin inactivation on localization of Kex2 protease are independent of the TGN localization signal in the cytosolic tail of Kex2p. Mol Biol Cell 7, 1667–1677.
Roberts CJ, Nothwehr SF, Stevens TH (1992). Membrane protein sorting in the yeast secretory pathway: evidence that the vacuole may be the default compartment. J Cell Biol 119, 69–83.
Scott PM, Bilodeau PS, Zhdankina O, Winistorfer SC, Hauglund MJ, Allaman MM, Kearney WR, Robertson AD, Boman AL, Piper RC (2004). GGA proteins bind ubiquitin to facilitate sorting at the *trans*-Golgi network. Nat Cell Biol 6, 252–259.
Seaman MN, Marcusson EG, Cereghino JL, Emr SD (1997). Endosome to Golgi retrieval of the vacuolar protein sorting receptor, Vps10p, requires the function of the VPS29, VPS30, and VPS35 gene products. J Cell Biol 137, 79–92.
Seeger M, Payne GS (1992). A role for clathrin in the sorting of vacuolar proteins in the Golgi complex of yeast. EMBO J 11, 2811–2818.
Shiba T *et al*. (2002). Structural basis for recognition of acidic-cluster dileucine sequence by GGA1. Nature 415, 937–941.
Sipos G, Brickner JH, Brace EJ, Chen L, Rambourg A, Kepes F, Fuller RS (2004). Soi3p/Rav1p functions at the early endosome to regulate

endocytic trafficking to the vacuole and localization of *trans*-Golgi network transmembrane proteins. Mol Biol Cell 15, 3196–3209.
Takatsu H, Katoh Y, Shiba Y, Nakayama K (2001). Golgi-localizing, gamma-adaptin ear homology domain, ADP-ribosylation factor-binding (GGA) proteins interact with acidic dileucine sequences within the cytoplasmic domains of sorting receptors through their Vps27p/Hrs/STAM (VHS) domains. J Biol Chem 276, 28541–28545.
Tan PK, Howard JP, Payne GS (1996). The sequence NPFXD defines a new class of endocytosis signal in *Saccharomyces cerevisiae*. J Cell Biol 135, 1789–1800.
Tomishige N, Noda Y, Adachi H, Shimoi H, Takatsuki A, Yoda K (2003). Mutations that are synthetically lethal with a gas1Delta allele cause defects in the cell wall of *Saccharomyces cerevisiae*. Mol Genet Genomics 269, 562–573.
Vojtek AB, Hollenberg SM, Cooper JA (1993). Mammalian Ras interacts directly with the serine/threonine kinase Raf. Cell 74, 205–214.
Wilcox CA, Redding K, Wright R, Fuller RS (1992). Mutation of a tyrosine localization signal in the cytosolic tail of yeast Kex2 protease disrupts Golgi retention and results in default transport to the vacuole. Mol Biol Cell 3, 1353–1371.
Zhu Y, Doray B, Poussu A, Lehto VP, Kornfeld S (2001). Binding of GGA2 to the lysosomal enzyme sorting motif of the mannose 6-phosphate receptor. Science 292, 1716–1718.